KU LEUVEN

FACULTY OF SCIENCE

The role of GARP on regulatory T cells and endothelial cells in cancer and angiogenesis

Sophie WAEGEBAERT

Supervisor: Prof. dr. H. Deckmyn
Laboratory for Thrombosis Research

Co-supervisor: *dr. W. Maes*
Laboratory for Thrombosis Research

Mentor: *E. Vermeersch*
Laboratory for Thrombosis Research

Thesis presented in
fulfillment of the requirements
for the degree of Master of Science
in Biochemie & Biotechnologie

Academic year 2016-2017

Acknowledgements

Five years of studying..., it seemed so long when I first set foot on Kulak ground. However, time goes by and I am already graduating! I have had an amazing time both in Kortrijk and Leuven.

This past year, I have spent a lot of time working on my master's thesis and I would not have been able to accomplish it without the help of some incredible people:

Thank you, professor Hans Deckmyn, for giving me the opportunity to work at the Laboratory of Thrombosis Research and for correcting my thesis.

Dr. Wim Maes, thank you very much for your comments that enhanced the level of my thesis. Your feedback helped me to think carefully about my results and to keep myself from trying to 'write a novel'.

Elien, what would this thesis have looked like without you? Thank you for correcting the first versions (and I know, that was sometimes a lot of work)! I am grateful for your help, your time, your motivation and knowledge, the many talks and your cheerfulness.

I also thank all the PhD students for helping me with little things and the good atmosphere in the lab. A special thank you for Elodie, for her explanations about the fluorescence microscope and for Senna, for helping me with the stainings, the NanoZoomer-SQ and Photoshop!

Nele, Inge and Aline, thank you for lending me a hand when necessary. Katleen, thank you for taking care of the mice and for the second opinions.

Hanne, Janne, Stijn, Laura and Sarah, thank you for the great time we had while we were writing our dissertations and for the nice chats during lunch-time. Hanne, thank you for being such a good friend and, not to forget, for the optimization of the staining protocols.

The biochemists of Kortrijk... Only four of us..., but that does not mean that we did not accomplish what we came for!

My parents, because you have given me the chance to study and to do the things I like to do and for supporting me. My sister Sarah for having lots of humor and an incredible talent for cooking and baking!

Emile, without your support and reassurance, I would not be who I am now.

To my other friends and family that I cannot mention in here: "Alone we can do so little; together we can do so much." - Helen Keller.

Summary

The transmembrane protein glycoprotein-A repetitions predominant protein (GARP) binds latent TGF-β and is expressed on several cell types, such as regulatory T cells (Tregs) and endothelial cells (ECs). Although the precise function of GARP in each context is elusive, it is known that TGF-β and Tregs are involved in cancer development, while TGF-β and ECs contribute to angiogenesis. The aim of this master's thesis is to identify the role of GARP on Tregs and ECs in cancer and angiogenesis.

MC38 cells and 3-methylcholanthrene (MCA) were injected in respectively endothelial (*Tie2*) and Treg (*Foxp3*) specific GARP knockout mice generated via the *Cre-LoxP* recombination system. Tumors were monitored and tumor infiltrating lymphocytes (TILs) were characterized in MCA tumors via flow cytometry. Treg functionality was also tested in an *in vivo* homeostasis model in immunodeficient mice. Angiogenesis was studied in *Tie2* specific GARP knockout mice via a wound healing assay in which wound closure was monitored and via the matrigel plug assay in which blood vessel formation was determined via immunohistochemistry.

Our results show that Treg GARP has no effect on tumor onset, TILs and Treg functionality. Strikingly, endothelial GARP had a significant effect on cancer progression: knockout mice showed a decrease in tumor volume. This could not be attributed to defects in angiogenesis, since wound closure and blood vessel formation were not different in knockout mice when compared to littermate mice.

We conclude that Treg GARP has no influence on cancer development. Whilst endothelial GARP seems not involved in blood vessel formation, it contributes to tumor growth.

Samenvatting

Het transmembraan eiwit GARP (*glycoprotein-A repetitions predominant protein*) bindt latent TGF-β en wordt onder andere tot expressie gebracht op regulatorische T-cellen (Tregs) en endotheelcellen (ECs). Ondanks het feit dat de functie van GARP op elk celtype nog niet volledig begrepen is, werd reeds bewezen dat TGF-β en Tregs betrokken zijn in kankerontwikkeling en dat TGF-β en ECs bijdragen tot angiogenese. In deze masterthesis wordt ingezoomd op de rol van GARP op Tregs en ECs in kanker en angiogenese.

MC38-cellen en 3-methylcholanthreen (MCA) werden geïnjecteerd in respectievelijk endotheel (*Tie2*) en Treg (*Foxp3*) specifieke GARP knock-out muizen die gegeneerd werden via het *Cre-LoxP* recombinatiesysteem. Tumoren werden opgevolgd en de tumor-infiltrerende lymfocyten werden bepaald in MCA-tumoren via flowcytometrie. Ook werd de Treg-functionaliteit getest in een *in vivo* homeostasemodel in immunodeficiënte muizen. Angiogenese werd onderzocht in *Tie2* specifieke GARP knock-out muizen via een wondgenezingsmodel waarbij dorsale wonden werden gemaakt om zo de genezing op te volgen. Ook werd het matrigel-plug-model uitgevoerd om zo bloedvatvorming te bepalen via immunohistochemie.

Onze resultaten tonen aan dat GARP op Tregs geen effect heeft op het ontstaan van tumoren, op de tumor-infiltrerende lymfocyten en op de Treg-functionaliteit. Opvallend zijn de resultaten die tonen dat GARP op ECs wel een significant effect heeft, daar de tumoren in knock-out muizen kleiner waren. Dit kon niet worden verklaard door een defect in angiogenese, want wondgenezing en bloedvatvorming waren identiek in knock-out en wild-type muizen.

We concluderen dat Treg GARP geen invloed heeft op kankerontwikkeling, terwijl GARP op endotheel veelbelovende resultaten heeft opgeleverd inzake tumorgroei, maar niet in angiogenese.

List of abbreviations

Ab	antibody
AIC	adaptive immune cell
APC	antigen presenting cell
BAMBI	BMP and activin receptor membrane bound inhibitor
Bcl-2	B-cell lymphoma 2
bFGF	basic fibroblast growth factor
bp	base pair
BSA	bovine serum albumin
$CD8^+$ T cell	cytotoxic T cell
$CD4^+$ Th cell	$CD4^+$ effector T cell
CP	cytoplasmic
CTLA-4	cytotoxic T lymphocyte-associated antigen 4
DMSO	dimethyl sulfoxide
EC	endothelial cell
EDTA	ethylenediaminetetra-acetic acid
FACS	fluorescent-activated cell sorting
FBS	fetal bovine serum
Foxp3	forkhead box protein P3
FS	forward scatter
GARP	glycoprotein-A repetitions predominant protein
gDNA	genomic DNA
GP	glycoprotein
GVHD	graft-versus-host disease
HCC	hepatocellular carcinoma
HSC	hepatic stellate cell
HUVEC	human umbilical vein endothelial cell
IIC	innate immune cell
IL	interleukin
IL-2R	interleukin-2 receptor
IPEX	immunodysregulation, polyendocrinopathy, enteropathy, X linked syndrome
KO	knockout
LAP	latency-associated protein
LM	littermate
LRR	leucine-rich repeats
LRRC32	leucine-rich repeat containing 32
LSEC	liver sinusoidal endothelial cell
MAP kinase	mitogen-activated protein kinase

MCA	3-methylcholanthrene
NGS	normal goat serum
NSG	NOD *scid* gamma
PBMC	peripheral blood mononuclear cells
PBS	phosphate buffered saline
PCR	polymerase chain reaction
PD-1	programmed death-1
PD-L1	programmed death-1 ligand
PEAR-1	platelet endothelial aggregation receptor-1
RGD	arginine-glycine-aspartate motif
rpm	revolutions per minute
RT	room temperature
s.c.	subcutaneous
SD	standard deviation
sGARP	soluble GARP
shRNA	short hairpin RNA
siRNA	short interfering RNA
SNP	single nucleotide polymorphism
SP	signal peptide
SS	side scatter
TBE	tris-borate-EDTA
TBS	tris-buffered saline
TDLN	tumour-draining lymph node
TGF-β	transforming growth factor beta
TIL	tumor infiltrating lymphocyte
TM	transmembrane
TRAIL-DR5	tumor-necrosis factor-related apoptosis inducing ligand death receptor 5
Treg	regulatory T cell
TSA	thrombus surface area
TTA	time to platelet adhesion
UTR	untranslated region
VEGF	vascular endothelial growth factor
VEGFR2	type 2 vascular endothelial growth factor receptor
VWF	von Willebrand factor
YFP	yellow fluorescent protein

Contents

Acknowledgements I
Summary II
Samenvatting III
List of abbreviations IV

Part I: Literature review & objectives 1

Chapter 1 - Glycoprotein-A repetitions predominant protein 2
1. Structure 2
2. The GARP receptor binds latent TGF-β 3
3. Functions of GARP 4
3.1. GARP on regulatory T cells 4
3.2. GARP on B cells 6
3.3. GARP on platelets and on endothelium 6
3.4. GARP on liver sinusoidal endothelial cells and hepatic stellate cells 8
3.5. GARP on mesenchymal stromal cells 8
Chapter 2 - Cancer 9
1. From immunosurveillance to immunoediting 9
1.1. Elimination 10
1.2. Equilibrium 10
1.3. Escape 10
2. Regulatory T cells 11
2.1. Regulatory T cell mediated suppression 11
2.2. Role of TGF-β in regulatory T cell mediated suppression 12
2.3. Regulatory T cell mediated suppression in the tumor microenvironment 12
2.4. GARP expression in the context of malignancy 13
3. Mouse models in oncoimmunology 14
3.1. Methylcholanthrene: A carcinogen-induced cancer mouse model 14
Chapter 3 - Angiogenesis 16
1. Angiogenesis in health 16
1.1. Sprouting angiogenesis 16
1.2. Modulation of angiogenesis 16
2. Angiogenesis in wound healing 17
3. In vivo models of angiogenesis 17
3.1. Matrigel plug assay 17
3.2. Wound healing assay 18
Chapter 4 - Objectives 19

Part II: Materials & methods 20

Chapter 1 - Genotyping of Foxp3 and Tie2 mice 21
1. Mice breeding 21
2. Genotyping of mice 21
Chapter 2 - In vivo homeostasis model 24
1. Isolation and immunostaining of splenocytes 24
2. Fluorescence-activated cell sorting of splenocytes 24
3. Injection of $CD4^+$ effector T and regulatory T cells into NOD scid gamma mice 26
4. Analysis of the homeostasis model 26
4.1. Flow cytometry analysis on spleen tissue 26
4.2. Cell counting and flow cytometry analysis on blood samples 26
4.3. Immunofluorescent staining on spleen tissue 27
Chapter 3 - The MCA tumor model 29
1. Induction of fibrosarcomas in regulatory T cell specific GARP knockout and littermate mice 29
2. MCA tumor isolation and flow cytometry analysis 29
Chapter 4 - The MC38 tumor model 32
1. Thawing of MC38 cell stocks 32
2. MC38 cell passage 32
3. Production of MC38 cell stocks 32
4. MC38 cell isolation and injection in endothelial specific GARP knockout and littermate mice 32
Chapter 5 - A wound healing and matrigel plug assay 33
1. Wound healing assay 33
1.1. Surgery 33
1.2. VWF-VIP staining on skin tissue sections 33
2. Matrigel plug assay 34
2.1. Subcutaneous injection and isolation of the matrigel plug 34
2.2. VWF staining 34
2.3. CD31 staining 35
2.4. Analysis of the matrigel plug sections 35
Chapter 6 - Statistics 36

Part III: Results 37
Chapter 1 - Role of GARP on regulatory T cells in cancer 38
1. Genotyping of Foxp3 mice 38
2. Mice lacking GARP in regulatory T cells are not resistant against MCA-induced fibrosarcomas 38

2.1. MCA-induced fibrosarcoma incidence and growth kinetics in specific GARP knockout and littermate mice are not significantly different 39
2.2. Tumor infiltrating lymphocytes in the fibrosarcomas are not significantly different in specific GARP knockout and littermate mice 40
3. GARP deficient regulatory T cells show no compromised suppressive capacity 41
Chapter 2 - Role of GARP on endothelial cells in cancer 45
1. Genotyping of Tie2 mice 45
2. Specific GARP knockout mice develop significant smaller MC38 tumors when compared to littermate mice 45
Chapter 3 - Role of GARP on endothelial cells in angiogenesis 47
1. Endothelial specific GARP knockout mice do not show a difference in blood vessel formation in the matrigel plug when compared to littermate mice 47
2. Endothelial specific GARP knockout mice do not show a difference in wound healing when compared to littermate mice 47
Part IV: Discussion & conclusions 51
References 58
Appendix A - Risk analysis A1
Appendix B - Breeding scheme A2

Part I: Literature review & objectives

Chapter 1 - Glycoprotein-A repetitions predominant protein

1. Structure

The glycoprotein-A repetitions predominant protein (GARP) or leucine-rich repeat containing 32 (LRRC32) protein was first described by Ollendorf *et al*. (1992). *Garp* is located in the 11q13.5q-q14.1 chromosomal region in humans and on chromosome 7F in mice. With 80% similarity, mouse and human *Garp* are highly homologous (Bekri *et al*., 1997; Ollendorff *et al.*, 1992; Roubin *et al*., 1996).

The *Garp* gene is composed of two coding exons encoding a transmembrane protein of 662 amino acids with a molecular mass of 72 kDa (Macaulay *et al.*, 2007; Ollendorff *et al*., 1994). The first exon contains a signal peptide and nine amino acids, while the second exon consists of the remaining coding sequence and the 3' untranslated region (UTR). Together, the exons give rise to a signal peptide, an extracellular domain of 20 leucine-rich repeats (LRRs), a transmembrane region and an intracellular domain of 15 amino acids (Figure 1) (Ollendorff *et al*., 1994).

Figure 1: Representation of GARP. GARP consists of a signal peptide (SP), 20 LRRs grouped in two segments and separated from each other by a proline-rich segment, a transmembrane (TM) region and a short cytoplasmic domain (CP) (adapted from Wang *et al*., 2008).

Since LRR is a structural motif, GARP shows conformational similarities with other proteins in the LRR superfamily. All these proteins have a common amino acid domain with the consensus sequence LXLXXNXLXXLXXXXLXXLXXL. In GARP, a proline-rich domain is found between the tenth and the eleventh LRR, which separates the two LRR segments (Figure 1) (Roubin *et al*., 1996).

Proteins of the LRR family act in several biological processes. For example, the toll-like receptor 2 acts in neurogenesis and innate immunity (Rolls *et al.,* 2007), while LRRC8 is involved in B cell development and LRRC8-like proteins promote proliferation and activation of lymphocytes (Kubota *et al*., 2004). Also, the members (GPIbα, GPIbβ, GPIX and GPV) of the glycoprotein Ib/IX/V (GPIb/IX/V) platelet receptor complex belong to the LRR family and are involved in the regulation of vascular processes (Andrews *et al*., 2003).

GARP is expressed in the lung, the kidneys, the heart, the liver, the pancreas and the skeletal muscles (Ollendorff *et al*., 1994). Analytical techniques revealed that expression of GARP is also detected in placental endothelial cells, human umbilical vein endothelial cells (HUVECs), regulatory T cells (Tregs), B cells, platelets and megakaryocytes (Macaulay *et al*., 2007; O'Connor *et al*., 2009; Roubin *et al*., 1996; Stanic *et al.*, 2015; Wang *et al*., 2008).

2. The GARP receptor binds latent TGF-β

GARP, expressed on the cell membrane of different cell types, binds latent transforming growth factor beta (TGF-β). The three isoforms of TGF-β form, together with the activins and the bone morphogenetic proteins, a superfamily of growth factors and cytokines. Members of the TGF-β superfamily are involved in development, wound healing, immunity and tissue homeostasis (O'Kane & Ferguson, 1997; Robertson & Rifkin, 2013).

TGF-β is synthesized and expressed as a precursor polypeptide consisting of a prodomain and a growth factor domain. Before secretion, disulfide bonds are formed between two polypeptides to make a homodimer. Next, the endoprotease furin convertase cleaves the prodomain at the processing signal. However, the prodomain remains non-covalently associated with TGF-β and is called the latency-associated protein (LAP). The secreted complex is known as the small latent TGF-β and has no biological activity (Robertson & Rifkin, 2013). This complex can bind to GARP (Shi *et al*., 2011; Wang *et al*., 2012).

GARP keeps TGF-β inactive by binding its latent form. The crystal structure of latent TGF-β bound to GARP is ring-like (Figure 2). Via disulfide bonds, the LAP domains make a ring around the two TGF-β monomers. GARP is also bound through disulfide linkages to LAP on the opposite side of the ring (Shi *et al*., 2011; Wang *et al.*, 2012).

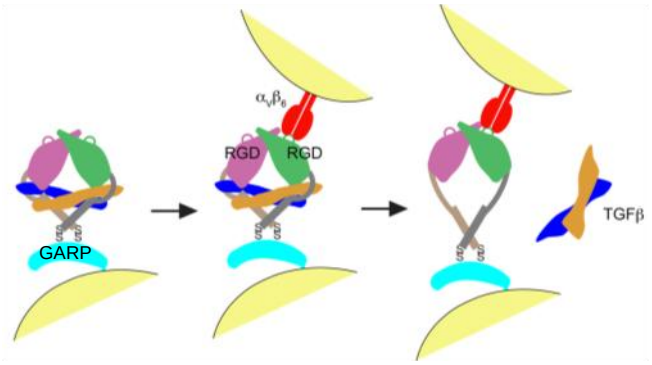

Figure 2: Representation of a possible activation mechanism of latent TGF-β from GARP. GARP (blue) expressed on the surface of a cell is disulfide linked to LAP (purple/green). Another cell expresses the integrin $\alpha_V\beta_6$ that binds the RGD motif in LAP. Together, GARP and $\alpha_V\beta_6$ create tensile force, which induces a conformational change in LAP and thus the release and the activation of TGF-β (adapted from Wang *et al*., 2012).

Release of TGF-β from LAP is necessary for its activation. Proteases, such as plasmin, cleave LAP, while thrombospondin-1 disrupts the non-covalent interactions between LAP and TGF-β in order to release an active form (ten Dijke & Arthur, 2007). Another activation mechanism involves the integrins $\alpha_V\beta_6$ and $\alpha_V\beta_8$. LAP contains the tripeptide arginine-glycine-aspartate (RGD motif), which is recognized by the integrins. However, recognition and binding of the RGD motif is not sufficient for activation. Membrane anchoring of GARP,

disulfide linkage between GARP and LAP and tensile force are also required to fully activate TGF-β (Figure 2) (Shi *et al.*, 2011; Wang *et al.*, 2012).

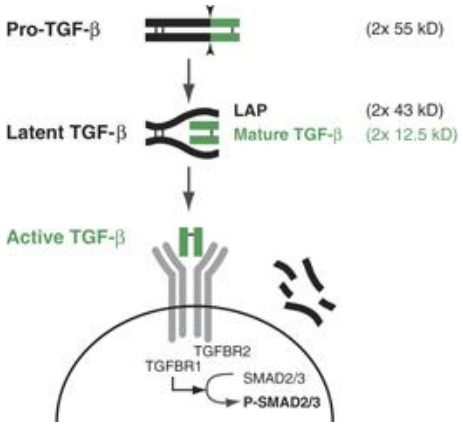

Figure 3: Schematic representation of TGF-β processing and signaling. The arrowheads indicate the site of proteolytic cleavage performed by furin convertase. The small bars show the position of the disulfide bonds. Once TGF-β is active, it induces a signal in the cell through receptor binding (TGFBR). Here, the signal is propagated through the canonical pathway involving Smad proteins (adapted from Stockis *et al.*, 2009a).

Once active, TGF-β binds its receptors TGFBR1 and TGFBR2, which are serine/threonine kinases (Figure 3). Gene transcription can be induced through the canonical pathway, which involves signal propagation via intracellular Smad proteins. However, gene transcription is also possible via the non-canonical pathway, which signals through mitogen-activated protein (MAP) kinases and GTPases. Both the canonical and non-canonical pathway activate genes involved in apoptosis, cell proliferation and migration (Massagué *et al.*, 2005; Moustakas & Heldin, 2005).

3. Functions of GARP

Besides earlier documented expression on Tregs, B cells, endothelial cells (ECs) and platelets, recent research indicates that GARP is expressed on a wider variety of different cell types, such as hepatic stellate cells and mesenchymal stromal cells (Carambia *et al*., 2014; Carrillo-Galvez *et al.*, 2015; Li *et al*., 2015; Macaulay *et al*., 2007; O'Connor *et al*., 2009; Roubin *et al*., 1996; Stanic *et al*., 2015; Stockis *et al*., 2009a).

3.1. GARP on regulatory T cells

Tregs are specialized peripheral immune cells, which inhibit T cell responses in order to avoid autoimmunity caused by self-reactive T cells. Tregs are characterized as $CD4^+CD25^+$ T cells expressing the transcription factor forkhead box protein P3 (Foxp3). Foxp3 is essential for the development and the suppressive capacity of Tregs. Mutation of Foxp3

induces severe autoimmunity and leads to immunodysregulation, polyendocrinopathy, enteropathy, X linked syndrome (IPEX) in humans (Sakaguchi, 2005).

In 2008, expression of GARP on the human Treg surface was shown by DNA microarray analysis and qPCR. GARP expression was more than 100 times higher in stimulated Tregs than in memory or naïve T cells. So, Tregs need to be stimulated through the T cell receptor before GARP expression is increased. The study also demonstrated that GARP is involved in the regulation of the suppressive activity of Tregs. Knockdown of GARP, using short hairpin RNA (shRNA), downregulated the suppressive activity as compared to control shRNA (Wang *et al.*, 2008). Next to activated human Tregs, a small fraction of resting murine Tregs also express GARP. After stimulation, GARP is upregulated (Edwards *et al*., 2013).

Experiments done with short interfering RNA (siRNA) suggest that latent TGF-β can directly bind to GARP on the Treg surface and that GARP is required for the surface expression of latent TGF-β (Tran *et al*., 2009). An increase in GARP expression enhances cleavage of pro-TGF-β and secretion of the latent complex. These processes are regulated by micro RNAs targeting the *Garp* 3' UTR (Gauthy *et al*., 2013).

However, the activation mechanism of latent TGF-β remains largely unknown. The absence of active TGF-β in culture supernatant of Tregs and effector T cell clones indicates that activation has to occur close to the Treg surface (Stockis *et al.*, 2009b).

Cuende *et al*. developed mouse anti-human GARP antibodies (Abs) that block TGF-β activation and the immunosuppressive capacity of human Tregs both *in vitro* and *in vivo*. To test the *in vivo* inhibition of Tregs, a xenogeneic graft-versus-host disease (GVHD) model was used, in which immunodeficient mice were injected with human peripheral blood mononuclear cells (PBMCs). Due to the xenotransplantation, the human T cells were reactive to murine tissue and induced GVHD. Nevertheless, co-injection with human Tregs delayed the onset of GVHD and showed the protective capacities of Tregs. Injection of an anti-GARP Ab accelerated GVHD and the onset of it was comparable with the injection of PBMCs without Tregs. These results show that anti-GARP Abs inhibit the immunosuppressive activity of human Tregs (Cuende *et al*., 2015).

These results show that GARP regulates the suppressive activities of Tregs. However, the observation that latent TGF-β/GARP complexes were detected in the culture medium of T cells transfected with GARP raised the question whether GARP has a regulatory function independent of Tregs (Gauthy *et al*., 2013). Hahn *et al.* engineered a soluble GARP (sGARP) protein and showed that sGARP not only inhibits the differentiation of naïve $CD8^+$ and $CD4^+$ T cells into their respective effector T cells, but also promotes the differentiation of naïve $CD4^+$ T cells into Tregs. Blocking TGF-β receptors diminished the effects. This demonstrates

that sGARP is able to act independently from Tregs and that its activity is regulated through TGF-β (Hahn *et al.*, 2013, 2016).

3.2. GARP on B cells

Expression of GARP has also been reported in B cells. B cells play an important role in the adaptive immune system by Ab production, antigen presentation and cytokine synthesis. B cells might also have a role in limiting excessive immune reactivity and at least a subset may act as regulatory B cells, which secrete the anti-inflammatory cytokine IL-10. IL-10 develops and maintains immune tolerance and homeostasis and is protective against excessive tissue damage caused by the host defense against pathogens. The suppressive activity of regulatory B cells is dependent on IL-10 secretion, but it is unknown how IL-10 affects the phenotype and the functions of regulatory B cells. Therefore, transgenic overexpression of IL-10 was established in human B cells. It was shown that IL-10 induces an immunoregulatory phenotype by the upregulation of GARP, among other molecules (Figure 4) (Stanic *et al*., 2015).

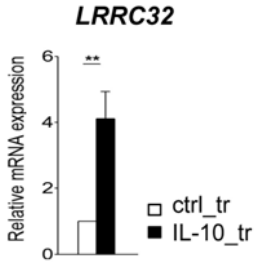

Figure 4: GARP expression is induced by IL-10 overexpression. GARP mRNA expression is significantly increased in B cells expressing transgenic IL-10 (ctrl_tr: control B cells; IL-10_tr: B cells expressing transgenic IL-10) (adapted from Stanic *et al*., 2015).

3.3. GARP on platelets and on endothelium

The Bloodomics Consortium was established to examine hematopoiesis and to identify genes involved in the functionality of the precursors of the different blood cell types. The gene expression pattern was compared between the cell types and all genes were collected in the HaemAtlas, which is a gene expression atlas for cells of the hematopoietic system (Watkins *et al*., 2009).

Whole-genome expression analysis performed on immune cells, erythroblasts and megakaryocytes showed that 279 genes were uniquely upregulated in megakaryocytes as compared to the other cell types. In a search for genes involved in thrombus formation, initially only genes encoding for transmembrane domains were selected. Transmembrane proteins are usually involved in cell functioning and can be more readily targeted for drug design. A list of 75 genes, with known and unknown functions, was obtained and further reduced by selecting genes with unknown functions in thrombosis, whether a reliable

zebrafish ortholog existed, whether interesting protein domains were present and whether there was expression in both megakaryocytes and ECs. Using these criteria, the genes *Garp, Bambi, Dcbld2* and *Esam* were identified. All were expressed in megakaryocytes and in HUVECs. Using flow cytometry and Western blot, it was shown that these proteins were also expressed in platelets (Figure 5) (Macaulay *et al*., 2007; O'Connor *et al*., 2009).

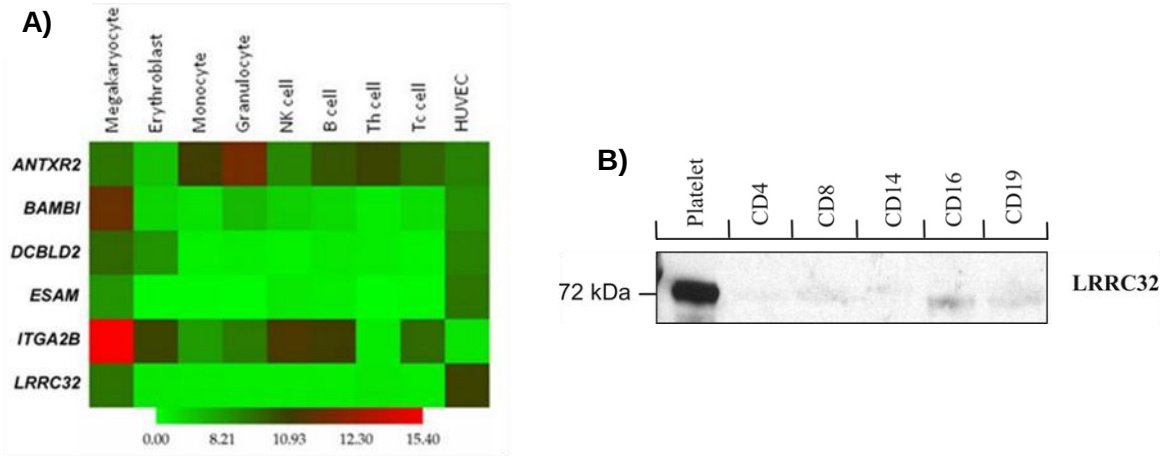

Figure 5: (A) Heatmap of normalized intensity values of megakaryocyte genes. *Antxr2* and *Itga2b* are included as positive controls. Increased expression of *Garp* was detected in megakaryocytes and in HUVECs (adapted from O'Connor *et al.*, 2009). **(B) Western blot of GARP distribution in purified populations of blood cells.** GARP expression is restricted to platelets (adapted from Macaulay *et al*., 2007).

Using a laser-induced thrombosis model in zebrafish, the selected genes, including *Garp*, were identified as having a role in thrombus formation and hemostasis. Genes were knocked down using antisense morpholinos. After induction of thrombosis and knockdown of *Garp* a significant defect in thrombus growth (29% decrease, $p = 0.034$) (Figure 6A) and a delay in platelet adhesion was detected (30% increase, $p = 0.051$) (Figure 6B) (O'Connor *et al*., 2009).

As shown in Figure 5A, *Garp* was not only expressed in platelets, but also in ECs (O'Connor *et al.*, 2009; Roubin *et al.*, 1996). Therefore, it was unclear whether the detected defect in thrombus growth in zebrafish was associated with the knockdown of *Garp* in platelets or in ECs, since morpholinos induce a full GARP knockdown (O'Connor *et al*., 2009).

Recently, the expression of GARP has also been confirmed on murine platelets and ECs. To determine the contribution of GARP in thrombus formation, platelet and endothelial specific GARP knockout mice were created, since full knockout mice were not viable. *In vitro* platelet function assays, *in vivo* thrombosis models and bleeding assays, however, could not show a role for GARP in hemostasis or thrombosis (Vermeersch *et al.*, 2017).

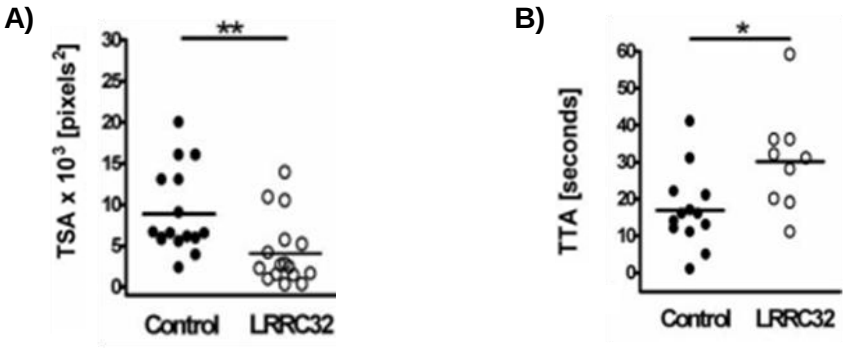

Figure 6: Effect of antisense knockdown of *Garp* on thrombus formation. (A) The thrombus surface area (TSA) of morpholino-injected zebrafish is compared to control zebrafish and shows a significant decrease in thrombus size (p = 0.034, decrease = 29%). **(B)** The time to platelet adhesion (TTA) is slightly increased in morpholino-injected zebrafish as compared to control zebrafish (p = 0.051, increase = 30%) (adapted from O'Connor *et al*., 2009).

3.4. GARP on liver sinusoidal endothelial cells and hepatic stellate cells

Besides its well characterized metabolic functions, the liver is also involved in immune tolerance and in inducing the conversion of peripheral non-Treg $CD4^+$ effector T ($CD4^+$ Th) cells into Tregs. The liver dendritic cells, the liver sinusoidal endothelial cells (LSECs) and the Kupffer cells are the main antigen presenting cells (APCs). All cell types are able to induce Tregs in a TGF-β dependent manner. However, LSECs are more potent in the induction of this differentiation of peripheral T cells into Tregs, since they express GARP, which is essential in presenting latent TGF-β on the cell surface. Active TGF-β is then used in the conversion of $CD4^+$ Th cells into induced Tregs (Carambia *et al*., 2014).

The liver also consists of hepatic stellate cells (HSCs), which, in a healthy liver, regulate the development and regeneration of liver tissue. Due to liver damage, HSCs become active and secrete TGF-β, which contributes to liver fibrosis. HSCs also inhibit activated T cells through the constitutive expression of the GARP/TGF-β complex. TGF-β suppresses proliferation and cytokine synthesis in active T cells. Blocking GARP decreases the suppressive activity of the HSCs (Li *et al*., 2015).

3.5. GARP on mesenchymal stromal cells

GARP expression is also detected in mesenchymal stromal cells. These cells are multipotent and have immunomodulatory characteristics, which are controlled through TGF-β expression. Activation and secretion of TGF-β on the cell surface is regulated via GARP, which enhances the immunoregulatory activities of the mesenchymal stromal cells. Therefore, GARP might represent a relevant marker for a better understanding of the mesenchymal stromal cell biology (Carrillo-Galvez *et al*., 2015).

Chapter 2 - Cancer

Cancer is caused by environmental and endogenous factors that induce DNA damage. Environmental factors, such as air pollution, asbestos, smoking and alcohol are big contributors to cancer development (Torre *et al*., 2015). Endogenous damage is caused by metabolic reactions that produce chemical intermediates which induce spontaneous DNA mutations and by DNA polymerases that are not flawless and incorporate non-complementary nucleotides during DNA replication (Loeb & Loeb, 2000).

In order to repair the damage, several DNA repair mechanisms exist. During DNA replication, the cell has to pass several checkpoints where possible mistakes might be repaired. However, if the mistake is irreparable, the cell undergoes apoptosis to avoid passing on harmful mutations to daughter cells. DNA repair and apoptosis are considered as intrinsic tumor suppressors (Vesely *et al.*, 2011). Despite the intrinsic suppressors, mutations in checkpoint proteins and the apoptosis pathway lead to escape from the cell cycle control and apoptosis, respectively. Consequently, inaccuracies are replicated and accumulated in the cell (Loeb & Loeb, 2000).

1. From immunosurveillance to immunoediting

In the late 1950s, the hypothesis of immunosurveillance was introduced that stated that cancerous cells that are not eliminated through the intrinsic tumor suppressors can be detected by the immune system, which is an extrinsic tumor suppressor. This implies that immune cells can eliminate transformed cells before they become cancerous (Burnet, 1957; Dunn *et al.*, 2004; Thomas, 1959).

Several laboratories reported the importance of immune cells in immunosurveillance. Cytotoxic T cells ($CD8^+$ T cells), natural killer cells, natural killer T cells and γδ T cells are all involved in the immunosurveillance and the protection of the host against carcinogenesis (Girardi *et al.*, 2001; Smyth *et al*., 2000a, 2000b).

However, observation of tumor development in immunocompetent and immunodeficient animals raised questions on the protective properties of the immune system as the cancer incidence in athymic nude mice was comparable to normal mice (Dunn *et al*., 2004). But, using tumor transplantation studies, it was shown that tumors raised in immunodeficient mice are more immunogenic than tumors from immunocompetent mice, since tumors grown in immunodeficient mice were rejected in wild-type mice. Tumor cells with reduced immunogenicity or with the capacity to suppress immune attacks have a higher chance of survival in the host (Dunn *et al.*, 2004; Shankaran *et al*., 2001).

Since tumors formed in the presence of an intact immune system are less immunogenic than tumors that develop in immunodeficient mice, it seems that the immune system promotes the growth of tumors that are able to escape immune detection. Hence, it is now proposed that

immunosurveillance is part of the process of immunoediting where immune cells are protective, but also shape the tumor immunogenicity (Shankaran *et al*., 2001). The concept of immunoediting is characterized by three phases, being elimination, equilibrium and escape (Dunn *et al*., 2004).

1.1. Elimination

The elimination phase represents the original concept of immunosurveillance. Innate immune cells (IIC) sense danger signals coming from the invading tumor. Recruitment of IICs leads to IFN-γ production, which amplifies the innate immune response. Due to induction of anti-proliferative and angiostatic signals and stimulation of apoptosis, some tumor cells die. Antigens coming from the dead tumor cells are taken up by dendritic cells and presented to adaptive immune cells (AIC) in the lymph nodes. Next, effector cells, mainly $CD4^+$ Th cells and cytotoxic $CD8^+$ T cells, invade and eliminate the tumor using direct and indirect mechanisms (Dunn *et al.*, 2004).

1.2. Equilibrium

However, not all tumor cells are eliminated and an equilibrium is established between the immune system and the tumor. The tumor cells that survived elimination form a heterogeneous tumor cell population in which some cells are dormant and other cells accumulate DNA mutations. Since lymphocytes and IFN-γ can only suppress the cancerous cells, more DNA mutations are acquired during the equilibrium phase and the heterogeneity of the tumor further increases. Consequently, the suppressive capacity of the immune system can be lost, the tumor will be able to escape the equilibrium phase and becomes detectable (Dunn *et al*., 2004).

Koebel *et al.* showed that only the adaptive immune system is involved in the equilibrium phase. They injected the chemical carcinogen 3-methylcholanthrene (MCA) in wild-type mice and monitored the growth of sarcomas during 200 days. One group of mice was treated with control Abs, a second group received a mixture of AIC-depleting Abs and a third group was injected with Abs against the IICs. Only mice of the second group developed sarcomas ($p = 0.0008$) (Koebel *et al*., 2007).

1.3. Escape

During the escape phase, tumor cells have gained several immunosuppressive mutations that make recognition by the immune system impossible. The immune system is no longer able to kill or control them. Instead, the tumor releases factors that inhibit both IICs and AICs and induces an immunosuppressive microenvironment in which Tregs and macrophages are attracted. These cells suppress other subsets of immune cells to obtain inhibition of the anti-tumor immune response. Furthermore, tumor cells become insensitive to IFN-γ and defects occur in antigen presentation. Consequently, tumor cells start to proliferate (Dunn *et al*., 2004).

2. Regulatory T cells

The physiological roles of Tregs are complex and involve tissue homeostasis and peripheral immune tolerance against self-antigens to avoid autoimmunity. However, when cancer evolves, Tregs inhibit the anti-tumor responses and, as a consequence, stimulate tumor growth (Oleinika *et al.*, 2013).

2.1. Regulatory T cell mediated suppression

Tregs have suppressive functions and regulate other immune cells through the expression of several cell-surface molecules and cytokines. An important molecule is CD25, a subunit of the interleukin-2 receptor (IL-2R) involved in binding the cytokine IL-2. IL-2R is upregulated in activated $CD4^+$ Th cells and constitutively expressed on Tregs. In that way, competition for IL-2 exists between the two cell types. Consumption of IL-2 by Tregs is necessary for their survival, since they cannot produce IL-2 by themselves as contrasted to $CD4^+$ Th cells. *In vitro*, IL-2 competition induces apoptosis in $CD4^+$ Th cells, caused by IL-2 deprivation. Consequently, Tregs suppress $CD4^+$ Th cells and thus modulate their growth and survival (Pandiyan *et al*., 2007).

CTLA-4 (cytotoxic T lymphocyte-associated antigen 4) is a key modulator of Treg function, since knockout of CTLA-4 induces multi-organ inflammation, allergies, autoimmune diseases and increased tumor immunity (Wing *et al*., 2008). The ligands of CTLA-4 are CD80 and CD86, which are expressed on APCs. Binding of CTLA-4 with CD80 or CD86 induces their downregulation through trans-endocytosis induced by the CTLA-4 expressing cell. On $CD4^+$ Th cells, the co-stimulatory molecule CD28 is competing with CTLA-4 for the ligands CD80 and CD86. Trans-endocytosis of CD80 and CD86 induced by CTLA-4 suppresses the $CD4^+$ Th immune responses (Qureshi *et al.*, 2011). Furthermore, CTLA-4 arrests the cell cycle, inhibits IL-2 synthesis by $CD4^+$ Th cells and reduces the interaction time between APCs and $CD4^+$ Th cells (Friedline *et al*., 2009; Tai *et al*., 2012).

The PD-1:PD-L1 pathway (programmed death-1 and programmed death-1 ligand) is also involved in the balance between stimulatory and inhibitory signals necessary for immunity and maintenance of self-tolerance. The functionality of dendritic cells expressing PD-1 is negatively regulated by Tregs expressing PD-L1 (Francisco *et al*., 2010). Interaction between PD-1 expressed on $CD4^+$ Th cells and PD-L1 on Tregs downregulates $CD4^+$ Th cell proliferation and cytokine production (Freeman *et al.*, 2000). PD-L1 expressed on APCs is also involved in the differentiation of naïve $CD4^+$ T cells that express PD-1 into induced Tregs (Francisco *et al*., 2009).

As previously described, activated Tregs express the transmembrane protein GARP, which binds latent TGF-β (Stockis *et al*., 2009a). Although the activation mode of TGF-β is not yet fully understood, Cuende *et al.* showed that GARP is required for TGF-β activation and thus

inducing the suppressive function of Tregs (Cuende *et al.*, 2015). Downregulation of GARP weakened the suppressive function of Tregs and inhibited the role of Tregs in the regulation of other $CD4^+$ Th cells (Probst-Kepper *et al.*, 2009; Tran *et al.*, 2009; Wang *et al.*, 2008).

In addition, Tregs also secrete inhibitory cytokines, such as IL-10, IL-35, IL-9 and TGF-β to regulate the immune system (Josefowicz *et al.*, 2012). Galectin-1, the tumor-necrosis factor-related apoptosis inducing ligand-death receptor 5 (TRAIL-DR5) pathway and the granzyme B or granzyme A pathways are cytolytic and induce apoptosis of $CD4^+$ Th cells (Garín *et al.*, 2007; Gondek *et al.*, 2005; Grossman *et al*., 2004; Ren *et al.*, 2007).

2.2. Role of TGF-β in regulatory T cell mediated suppression

Tregs are able, depending on the strength of T cell receptor stimulation, to produce secreted and cell surface-bound TGF-β (Nakamura *et al*., 2004). TGF-β is an immunoregulatory cytokine with an influence on T cell proliferation, differentiation and survival.

In vitro data were contradictory and do not include, nor exclude TGF-β in the mediation of the suppressive role of Tregs (Piccirillo *et al*., 2002). In contrast, *in vivo* studies do show the significance of TGF-β, since Tregs are only able to suppress the onset of inflammatory bowel disease and induce recovery from allergic encephalomyelitis through secretion of TGF-β. Inhibition of TGF-β eliminates these suppressive roles (Li *et al*, 2007; Zhang *et al*., 2006).

The role of TGF-β in tumor development is complex. TGF-β has both promoting and inhibitory functions in the tumor microenvironment. This is known as the TGF-β paradox (Tian & Schiemann, 2009). In the early phase of the tumor, TGF-β suppresses tumor development through apoptosis, arrest of the cell cycle and prevention of cell immortalization (Datto *et al.*, 1995; Korah *et al.*, 2012; Lacerte *et al.*, 2008; Li *et al.*, 1995). TGF-β suppression is lost when inactivating mutations occur in the TGF-β receptors or Smad genes. Consequently, cancer cells are no longer inhibited by TGF-β and colon, gastric, breast and glioma cancerous cells are stimulated to grow (Chen *et al*., 1998; Fleming *et al.*, 2013; Grady *et al.*, 1999; Izumoto *et al*., 1997; Park *et al.*, 1994; Sun *et al.*, 1994).

2.3. Regulatory T cell mediated suppression in the tumor microenvironment

When cancer cells escape immunosurveillance through selection of less immunogenic cells, an immunosuppressive environment is established (Dunn *et al*., 2004). Although the tumor is able to escape the control of the immune system, lymphocytes can still invade the tumor. These immune cells are known as the tumor infiltrating lymphocytes (TILs). The different types of T lymphocytes have several functions in the tumor environment. $CD8^+$ T cells directly kill tumor cells, while $CD4^+$ Th cells are a heterogeneous cytokine-secreting group and Tregs are involved in the suppression of $CD4^+$ Th cells (Yu & Fu, 2006). Depending on the type and the amount of immune cells present in the TILs, correlations can be made between TILs and patient outcome. Presence of $CD4^+$ and $CD8^+$ T cells in advanced disease

indicated a 5-year survival of 38% of ovarian cancer patients. In contrast, absence of $CD4^+$ and $CD8^+$ T cells resulted in a survival of only 4.5% (Zhang *et al*., 2003). When looking at the subtypes of T cells, less Tregs (12%) were found in tumor biopsies from patients with stage I disease as compared to stage II-IV disease (25-30%) (Curiel *et al*., 2004). In conclusion, it seems that a higher $CD8^+$/Treg ratio correlates with a significant higher survival of ovarian cancer patients (Sato *et al*., 2005).

Unfortunately, the suppressive mechanisms of Tregs described above also contribute to the tolerance against tumors. As cancer progresses, Treg enrichment in the tumor environment is established through tumor-derived chemokines and microenvironmental macrophages that promote migration of Tregs to the tumor (Curiel *et al*., 2004). In the tumor, Tregs inhibit other infiltrating immune cells through secretion of TGF-β and other cytokines, expression of cell surface proteins and cytolysis of immune cells (Oleinika *et al*., 2013). Additional to their suppressive role, Tregs synthesize vascular endothelial growth factor (VEGF), which promotes angiogenesis. Vessel formation is essential for the tumor to get access to nutrients and growth factors (Facciabene *et al*., 2011).

2.4. GARP expression in the context of malignancy

GARP can also be expressed in some cancer tissues, such as breast cancer and melanoma. In other cancers, such as hepatocellular carcinoma (HCC), colon and ovarian cancer, tumor infiltrating Tregs show a rise in GARP expression. This contributes to an increase of the immunosuppressive activities induced by the tumor (DeRycke *et al*., 2013; Hahn *et al*., 2016; Kalathil *et al.*, 2013; Metelli *et al.*, 2016; Pastille *et al*., 2014).

A recent study of Metelli *et al.* showed a significant increase of GARP in breast cancer tissues of patients. To determine the role of GARP in the tumor microenvironment, carcinoma cell lines were transfected with GARP. Injection of these cancer cells in immunodeficient mice induced an increase in tumor size, metastasis and signaling of the canonical TGF-β pathway. GARP expressing cancer cells were also two to three times more efficient in inducing Treg differentiation as compared to control cells and were able to stimulate Treg migration to the tumor microenvironment (Metelli *et al*., 2016).

This shows that GARP expression in cancer can represent an important factor contributing to oncogenesis and immune tolerance, since it promotes the establishment of primary tumors, metastasis and the induction of Tregs in the tumor microenvironment (Metelli *et al*., 2016)

Patients with HCC, a type of liver cancer, have increased levels of Tregs. Also, Tregs in advanced stage HCC patients have significant elevated expression of GARP and are thus more immunosuppressive (Kalathil *et al.*, 2013). In parallel, in a mouse model of colitis-associated colon cancer, more GARP positive Tregs were found in mice with colon cancer as compared to control mice (Pastille *et al*., 2014).

Tregs are also involved in ovarian cancer. Research on single nucleotide polymorphisms (SNPs) that influence the functionality of Tregs found a SNP in GARP in ovarian cancer patients. The SNP elevates GARP stability and expression levels on Tregs. Consequently, the immunosuppressive phenotype of the Tregs is increased, which lowers the chances of survival of ovarian cancer patients (DeRycke *et al*., 2013).

In addition to the expression of GARP on both Tregs and cancer cells, GARP can also be shed from the cell surface from melanoma cells to form sGARP. sGARP contributes to the tumor microenvironment by inhibiting $CD4^+$ Th cells, inducing Tregs and activating tumor-associated macrophages (Hahn *et al.*, 2016). Moreover, it was shown that the platelet GARP/TGF-β complex is involved in the suppression of immune cells invading the tumor and thus in promoting tumor growth (Rachidi *et al*., 2017).

3. Mouse models in oncoimmunology

To better understand the role of the immune system in tumor development and the design of therapeutic drugs, distinct experimental tumor models in mouse are used.

3.1. Methylcholanthrene: A carcinogen-induced cancer mouse model

Carcinogens are used to induce local tumors, which are easily monitored. After application of the carcinogens, 'natural' oncogenesis is induced, which is used to understand the relationship between the immune system and the transforming cells in the early stage of cancer development (Betts *et al.*, 2007; Zitvogel *et al*., 2016).

MCA is a polycyclic aromatic hydrocarbon. After enzymatic metabolism, its metabolites bind DNA and induce random mutations. Mutations in proto-oncogenes and tumor suppressor genes transform cells and allow tumors to develop. MCA induces malignant soft tissue sarcomas, called fibrosarcomas that are composed of fibroblasts (Qin *et al*., 2002). Using this model, Betts examined the influence of Tregs on MCA-induced sarcogenesis (Betts *et al.*, 2007).

Approximately 70 to 80% of mice injected with MCA developed fibrosarcomas by week 29 after injection. Using histology, it was shown that tumors were infiltrated with lymphocytes and that almost half of the $CD4^+$ fractions is $Foxp3^+$ and thus regulatory. These Tregs were found in close proximity of $CD4^+$ Th and $CD8^+$ T cells, which were located at the border between tumor and healthy tissue (Figure 7). This indicates a continuous immune response, which is controlled via Tregs among others. Tregs were present in the TILs and significantly enriched in tumor-draining lymph nodes (TDLNs) as compared to non-TDLNs. This might imply that, in the case of tumor-specific immune activity, Tregs expand (Betts *et al*., 2007).

MCA injected in mice depleted of Tregs and in control mice showed that the tumor incidence in the control group was higher than in the mice without Tregs (Figure 7). Together, these results show that Tregs suppress immunosurveillance of carcinogen-induced tumors in immunocompetent mice (Betts *et al*., 2007).

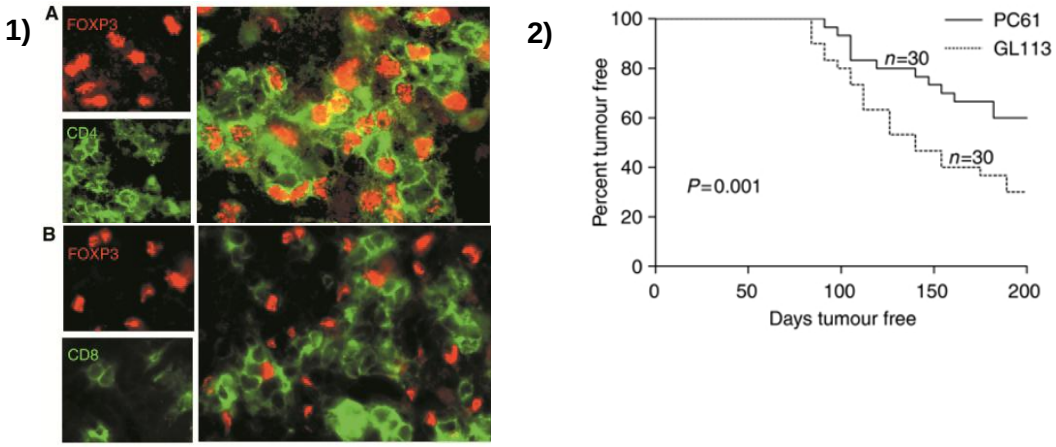

Figure 7: Enrichment of Tregs and tumor incidence in MCA-treated mice. **(1)** Sections of MCA-induced tumors are stained with anti-Foxp3-specific Ab (red) and (A) anti-CD4 or (B) anti-CD8 Ab (green). **(2)** Mice were treated with either PC61 to deplete Tregs or GL113 as a control Ab. Nine out of 30 control mice remained tumor free, while 18 out 30 mice depleted of Tregs did not develop a tumor (adapted from Betts *et al.*, 2007).

3.2. MC38: A syngeneic mouse tumor model

The MC38 cell line is established from colon adenocarcinoma cells which were developed in C57BL6 mice. The model can be used to determine the identity of the TILs in the tumor microenvironment, since the implanted cells are immunologically compatible with the murine immune system and thus syngeneic (Budhu *et al.*, 2014).

It is shown that Tregs are significantly upregulated in the spleen, the TDLNs and the MC38 tumor itself. Just as in the above described MCA model, proliferation of lymphocyte populations with antitumoral activity is suppressed by the Tregs (Budhu *et al.*, 2014; Medina-Echeverz *et al*., 2011).

Also, MC38 cells have lost Smad4 signaling, which is a signaling pathway induced by TGF-β. Consequently, TGF-β switches from tumor suppressing to tumor promoting. Re-expression of Smad4 signaling reduces tumor growth and restores the tumor suppressing role of TGF-β (Zhang *et al*., 2010).

Chapter 3 - Angiogenesis

1. Angiogenesis in health

Blood vessels connect the different organs of the body and are involved in nutrient and oxygen supply, removal of waste products and immunosurveillance. In that way, tissue homeostasis and health are obtained (Carmeliet & Jain, 2011).

De novo formation of blood vessels or vasculogenesis only occurs in the embryo. This differs from angiogenesis, which is the formation of blood vessels from pre-existing blood vessels. Angiogenesis is involved in normal repair processes in the body, but also in pathologies, such as in cancer (Carmeliet & Jain, 2011).

Blood vessels are composed of a monolayer of ECs lining the lumen, surrounded by a basement membrane and subsequent layers of mural cells (smooth muscle cells and pericytes). ECs are quiescent cells, but due to circumstances such as tissue damage, low oxygen or nutrient levels and cancer, pro-angiogenic signals are released. ECs will lose their cell-cell contacts, start to proliferate, migrate and differentiate into new blood vessels in a process called sprouting angiogenesis (Carmeliet & Jain, 2011).

1.1. Sprouting angiogenesis

Angiogenesis involves the differentiation of ECs into tip and stalk cells. Tip cells sense angiogenic signals through their filopodial extensions, while stalk cells play a supportive role in the extension of sprouting vessels. Stalk cells establish the vascular lumen and keep the new vessel in contact with the parental vessel. Thus, the tip cell guides, while the stalk cell proliferates and elongates the sprout. Proliferation and elongation continue until two tip cells fuse with each other to form a new circuit. Next, the lumen is established and mural cells are recruited via growth factors. Once the blood vessel is formed, ECs become quiescent and differentiate into the phalanx phenotype forming a tight barrier which makes blood flow possible (Potente *et al*., 2011).

Determination of tip and stalk cells is dependent on the sensitivity of the ECs for VEGF and the presence of its receptor, the type 2 VEGF receptor (VEGFR2) (Gerhardt *et al.*, 2003). VEGF expression is increased in ECs to induce angiogenesis in hypoxic tissues, and thus to restore oxygen and nutrient supply (Liu *et al.*, 1995). VEGF signaling involves several downstream pathways, such as MAP kinases, phospholipase Cγ and small GTPases, through which EC proliferation and migration, development of filopodia and degradation of the extracellular matrix is made possible (Herbert & Stainier, 2011).

1.2. Modulation of angiogenesis

Angiogenesis is a complex process, which is regulated through several signals. Important players are VEGF and TGF-β. Both have different functions in the induction of angiogenesis and the role of TGF-β in angiogenesis is not yet completely understood. The sometimes

opposing functions of TGF-β are illustrated by studies performed *in utero*, *in vitro* and *in vivo* (Ferrari *et al*., 2006, 2009, 2012).

In utero, TGF-β deficient mice die prenatally and have defective vasculogenesis. *In vitro*, TGF-β inhibits EC proliferation, induces EC apoptosis and downregulates VEGFR2, while *in vivo* angiogenesis is induced both indirectly and directly through VEGF and the type 1 TGF-β receptor (Ferrari *et al.*, 2009).

For several years, research has been done to unravel the regulatory mechanisms of angiogenesis and apoptosis. Apoptosis is a valuable mechanism in the formation of healthy blood vessels and the progress of angiogenesis, since inhibition of apoptosis results in abnormal vessels. Ferrari *et al.* found a relation between VEGF and TGF-β in regulating cell proliferation on the one hand and apoptosis on the other (Ferrari *et al*., 2006, 2009, 2012).

TGF-β regulates apoptosis as well as angiogenesis through mediation by VEGF and through downregulation of the anti-apoptotic protein Bcl-2 (B-cell lymphoma 2) (Tsukada *et al.*, 1995). Induction of angiogenesis is only possible when apoptosis is fast and transient. In conclusion, angiogenesis can only proceed when the optimal level of apoptosis is reached (Ferrari *et al*., 2009).

2. Angiogenesis in wound healing

Injury to the skin induces a range of processes in order to induce wound healing and to avoid possible microbial infections. Wound healing is characterized by blood clotting, inflammation and formation of new tissue through proliferation, angiogenesis and tissue remodeling. These steps have to be followed chronologically in order to restore vasculature. During wound healing, temporal and spatial regulation is needed between ECs, angiogenic growth factors and molecules of the extracellular matrix (Eming *et al.*, 2007).

The formation of a blood clot following injury is necessary to prevent micro-organisms from entering the tissue, but also as an attachment site for degranulated platelets and invading immune cells, serving as a source of growth factors and cytokines. Platelets are a major source of TGF-β and its release, together with other growth factors and cytokines, initiates the healing process (Eming *et al.*, 2007).

3. In vivo models of angiogenesis

Several models are developed to study angiogenesis and to screen pro- and anti-angiogenic compounds.

3.1. Matrigel plug assay

The matrigel plug assay is an *in vivo* assay used to test biological components and drugs for their effect on angiogenesis. The matrigel is a derivative of the Engelbreth-Holm-Swarm tumor composed of basement membrane proteins (Malinda, 2009). In the assay, an

angiogenic stimulus is added to the matrigel, followed by subcutaneous injection in mice. From then on, the matrigel gelifies and recruits ECs into the plug for the formation of vessels (Guillot *et al*., 2012; Malinda, 2009).

The matrigel assay was used to determine the role of the endothelial cell protein BAMBI (BMP and activin receptor membrane bound inhibitor) in angiogenesis. It is a competitive receptor of the type 1 TGF-β receptor. It was shown that *BAMBI*$^{-/-}$ mice have higher levels of angiogenesis as compared to *BAMBI*$^{+/+}$ mice, which indicates that BAMBI is important in the regulation of normal development of blood vessels (Guillot *et al*., 2012).

3.2. Wound healing assay

Another model to study angiogenesis is the wound healing assay. In the model, dorsal skin wounds are made and, during a certain period, wound closure, morphological architecture and degree of neovascularization are studied. The model has recently been used to study the role of the platelet endothelial aggregation receptor-1 (PEAR-1) on EC proliferation, migration and tube formation (Vandenbriele *et al.*, 2015).

Chapter 4 - Objectives

Since the first description of GARP as a transmembrane protein in 1992, research has shown that GARP expression is no longer limited to platelets, ECs and Tregs, but has expanded towards B cells, hepatic stellate cells and mesenchymal stromal cells (Macaulay *et al*., 2007; O'Connor *et al*., 2009; Roubin *et al*., 1996; Stanic *et al*., 2015; Wang *et al.*, 2008).

However, more questions than answers exist about the exact functions of GARP and the activation mechanisms of its ligand latent TGF-β. Therefore, three objectives were set in this master's thesis.

First, the function of GARP on Tregs in the development of cancer was determined, since previous studies have shown that GARP expressed on Tregs contributes to the suppressive activities of Tregs and that GARP expressing Tregs are upregulated in certain cancer types (Cuende *et al*., 2015; Kalathil *et al*., 2013; Pastille *et al*., 2014). To test this, the carcinogen MCA was injected into the hind legs of Treg specific GARP knockout and littermate mice. Tumors that developed were measured and the TILs present in the tumor were determined in order to compare tumor incidence, tumor growth, tumor onset and immune cell populations present in the tumor. Next, an *in vivo* homeostasis model was also performed to compare the functionality of Tregs expressing and not expressing GARP in a tumor-free environment.

Second, endothelial GARP was also of interest in the development of cancer, since Carambia *et al.* have shown that GARP expressed on LSECs contributes to the differentiation of effector T cells into Tregs (Carambia *et al*., 2014). Endothelial specific GARP knockout and littermate mice were compared to each other by subcutaneously injecting cells of the MC38 cell line into the ventral region. Tumor development was followed for 40 days and every two days, tumors were measured to determine a possible difference in tumor growth.

Finally, the role of endothelial GARP in angiogenesis was also determined. Studies of O'Connor and Vermeersch already showed that GARP is expressed on the endothelium, which might be necessary for TGF-β activation, followed by regulation of angiogenesis (O'Connor *et al.*, 2009; Vermeersch *et al*., 2017). To test this hypothesis, wound healing and matrigel plug assays were performed in endothelial specific GARP knockout and littermate mice.

Part II: Materials & methods

Chapter 1 - Genotyping of *Foxp3* and *Tie2* mice

1. Mice breeding

Cell specific knockout mice were created via the *Cre/LoxP* recombination system. This system requires both a *Cre* mouse strain, in which the *Cre* recombinase is expressed under the control of a tissue specific promoter and a *LoxP*-containing mouse strain, in which the target gene is flanked by *LoxP* sites. Crossing the mouse strains generates offspring with a cell specific gene knockout, since the *Cre* recombinase recognizes the sequence motif of the *LoxP* site and excises the target gene (Kos, 2004).

Tie2 (courtesy of M. Yanagisawa, Southwestern Medical School, Dallas, TX) and *Foxp3* (courtesy of A. P. Rudensky, Howard Hughes Medical Institute, Immunology Program, Ludwig Center, Memorial Sloan-Kettering Cancer Center, New York, NY) promoter-driven *Cre* recombinase transgenic mice were used to delete the target gene *Garp* in ECs and Tregs, respectively. *Tie2* and *Foxp3* specific GARP knockout mice were obtained through mating *Cre* recombinase transgenic mice with the $Garp^{fl/fl}$ mice, followed by backcrossing of $Cre^{+/-}$, $Garp^{fl/-}$ mice with $Garp^{fl/fl}$ mice to obtain $Cre^{+/-}$, $Garp^{fl/fl}$ (knockout) and $Cre^{-/-}$, $Garp^{fl/fl}$ (littermate) mice (see Appendix B for breeding scheme). Due to cell specific *Cre* recombinase expression in *Tie2* and *Foxp3* mice, the first exon of *Garp* is cut out of the genome of the Treg and ECs and completely disrupts *Garp* expression (Edwards *et al.*, 2014; Rubtsov *et al.*, 2008; Vermeersch *et al.*, 2017). In experiments concerning *Foxp3* mice, only male mice were used since the *Foxp3* gene is located on the X chromosome, while both male and female mice were used of the *Tie2* knockout mice.

2. Genotyping of mice

To determine the genotype of the *Foxp3* and *Tie2* specific GARP knockout mice and their littermates, the polymerase chain reaction (PCR) was performed on genomic DNA (gDNA). For the generation of transgenic mice expressing *Cre* recombinase under the *Foxp3* promoter, a construct was made in which *Cre* was fused to yellow fluorescent protein (YFP). This construct was knocked in in the 3'UTR of the *Foxp3* locus. When the *Cre* recombinase is active, YFP expression can be detected, which can be used for cell sorting, flow cytometry analysis and genotyping (Rubtsov *et al*., 2008).

gDNA was extracted from ear samples with the NaOH extraction method. Therefore, each ear sample received 75 µL work solution (Table 1). Samples were placed in the Thermomixer Comfort (Eppendorf, Rotselaar, Belgium) and stirred for 10 minutes at 1400 rpm and 95°C. Next, samples were placed for 10 minutes at 4°C. Finally, the work solution was neutralized with 75 µL TrisHCl pH 5. Following gDNA extraction, the master mix, which contains all components required for the PCR, was prepared in a DNA free environment and 5 µL gDNA was added to each PCR Eppendorf tube containing the master mix (Table 2).

Table 1: Composition work solution NaOH extraction method.

Component	Supplier
0.5 M NaOH	Fisher Chemicals Merelbeke, Belgium
0.5 M Na_2EDTA	Fisher BioReagents, Merelbeke, Belgium
dH_2O	-

Table 2: Composition master mix for one sample.

Component	Volume	Supplier
10x PCR buffer	2.5 µL	All from Invitrogen, Ghent, Belgium
50 mM $MgCl_2$	1.25 µL	
Primer forward	1 µL	
Primer reverse	1 µL	
10 mM dNTP mix	0.625 µL	
Platinum Taq polymerase	0.1 µL	
dH_2O	14.525 µL	-
Total	**21 µL**	

Table 3: PCR protocol. Denaturation, annealing and synthesis were repeated 30 times.

	Foxp3-Cre	***Tie2-Cre***	***Garp LoxP***
Initial denaturation	2', 95°C	2', 95°C	2', 95°C
Denaturation	30'', 95°C	30'', 95°C	30'', 95°C
Annealing	30'', 62°C	30'', 62°C	30'', 55°C
Synthesis	30'', 72°C	30'', 72°C	30'', 72°C
Elongation	10', 72°C	10', 72°C	10', 72°C
Forever	12°C	12°C	12°C

After adding the master mix, DNA was amplified using PCR (PTC-200 Thermal Cycler, Bio-Rad Laboratories Inc, CA) (Table 3) with four different pairs of primers for *LoxP*, *Cre* driven by *Tie2*, *Cre* driven by *Foxp3* and internal HIF700 and HIF960 control primers used for genotyping of *Tie2* specific GARP knockout mice (Table 4).

DNA analysis was performed via gel electrophoresis. To analyze the presence or absence of *Cre,* an 1.5% agarose gel with Gelgreen Nucleic Acid Stain was made (1/10 000 dilution, Biotium, CA), while for *LoxP*, a 2% agarose gel with Gelgreen Nucleic Acid Stain was prepared (1/10 000 dilution). The agarose gel was made with UltraPure Agarose (Invitrogen, Ghent, Belgium) dissolved in tris-borate-EDTA buffer (TBE, 0.5x, Table 5), which was heated until the solution boiled. Then, the solution was poured into a gel tray with the well comb in place and stored at room temperature (RT) until the gel was solidified. Before running the agarose gel, 5 µL loading dye (6x, Table 6) was added to the samples and a 100 base pair

(bp) molecular weight ladder (8 µL mQ; 2 µL 100 bp molecular weight ladder New England Biolabs, MA; 2 µL 6x loading dye) was prepared. The electrophoresis apparatus was filled with TBE (0.5x) and 20 µL of each sample was loaded into the gel. Electrophoresis was performed at 135 V. To detect the DNA, the gel was put under UV light (BioDoc-IT Imaging System, Ultra-Violet Products, Cambridge, UK).

Table 4: Sequence of primer pairs of *LoxP*, *Cre* driven by *Tie2* and *Cre* driven by *Foxp3* and internal control primers HIF700 and HIF900 used in the genotypic analysis.

Primer	Sequence
LoxP	5’-GCA AAG CAG ACG GTC ATA CA-3’
	5’-TCT GGA ACT CAA GAG GCT GAG-3’
Cre driven by *Tie2*	5’-CGC CGT AAA TCA ATC GAT GAG TTG CTT C-3’
	5’-GAT GCC GGT GAA CGT GCA AAA CAG GCT C-3’
Internal primer HIF700	5'-CAA GCA TTC TTA AAT GTG GAG CTA TCT-3'
Internal primer HIF960	5'-TTG TGT TGG GGC AGT ACT GGA AAG ATG-3'
Cre driven by *Foxp3*	5'-AGG ATG TGA GGG ACT ACC TCC TGT A-3'
	5'-TCC TTC ACT CTG ATT CTG GCA ATT T-3'

Table 5: Composition TBE buffer (10x, pH 8.3).

Component	Supplier
0.90 M Tris	Sigma Aldrich, St. Louis, Mo
0.90 M H_3BO_3	Acros Organics, Geel, Belgium
0.022 M Na_2EDTA	Fisher Bioreagents, Merelbeke, Belgium
dH_2O	-

Table 6: Composition loading dye (6x).

Product	Supplier
40% sucrose	Acros Organics, Geel, Belgium
0.25% bromophenol blue	Acros Organics, Geel, Belgium
10 mL dH_2O	-

Chapter 2 - *In vivo* homeostasis model

1. Isolation and immunostaining of splenocytes

The spleens of male *Foxp3* specific GARP knockout and *Foxp3-Cre* mice were isolated in a laminar flow cabinet after the mice were killed by cervical dislocation. The spleen was washed in PBS (phosphate buffered saline, Table 7) and cut into pieces. Using a 70 µm nylon cell strainer (Greiner Bio-One, Vilvoorde, Belgium) a single cell suspension was made, which was washed in PBS and centrifuged at 400 g for five minutes.

Erythrocytes were lysed by adding 5 mL of the erythrocyte lysis buffer for four minutes at RT (Table 8), followed by neutralization with 30 mL PBS. The suspension was centrifuged at 400 g for 10 minutes to remove the lysis buffer. After resuspending the cells in PBS, cells were counted with the Hemavet 950FS (Drew Scientific, Cumbria, UK).

Splenocytes were stained with anti-mouse CD4-PE (eBioscience, Vienna, Austria, clone GK1.5) and incubated for 20 minutes at 4°C. The non-bound Ab was removed by adding PBS and centrifugation at 400 g for five minutes. Cells were diluted in PBS to gain $3.00 \cdot 10^6$ cells/mL.

Table 7: Composition PBS buffer (10x, pH 6.5).

Product	Supplier
1.37 M NaCl	Carl Roth GmbH + Co. KG, Karlsruhe, Germany
0.027 M KCl	Merck, Darmstadt, Germany
0.065 M $Na_2HPO_4.2H_2O$	Sigma Aldrich, St. Louis, Mo
0.015 M KH_2PO_4	Acros Organics, Geel, Belgium
dH_2O	-

Table 8: Composition erythrocyte lysis buffer.

Product	Supplier
0.016 M NH_4Cl	Sigma Aldrich, St. Louis, Mo
0.010 M $NaHCO_3$	Acros Organics, Geel, Belgium
dH_2O	-

2. Fluorescence-activated cell sorting of splenocytes

Fluorescence-activated cell sorting or FACS is based on flow cytometry and allows to collect individual cells from single cell suspensions. As opposed to FACS, flow cytometry is only able to identify cell populations and uses the light-scattering characteristics of single cells to identify different cell types in a heterogeneous cell population. Briefly, a single cell suspension is taken up in a liquid stream that passes through a laser beam. Cells passing the laser beam emit light in all directions. Light scattered in the forward direction (forward scatter, FS) is used to determine cell size, while side-scattered (SS) light measures

granularity. Cells carrying fluorochromes emit fluorescent signals and are detected by fluorescence detectors. Together, FS, SS and fluorescent emissions are used to determine the characteristics of certain cell types in the single cell suspension. In addition to FS, SS and fluorescence labels to identify cell populations, FACS can isolate certain cell types via the generation of single droplets which contain the cells of interest. These droplets are electrically charged and, via an electrical field, redirected in order to collect the droplets. Cells present in the droplet can then be used again in experiments (Macey, 2007).

By using the FACSAria IIu (BD, Erembodegem, Belgium) of the KU Leuven FACS Core, the splenocytes were sorted to gain the $CD4^+$ Th and Treg cells expressing GARP and Treg cells knockout for GARP. Treg specific GARP knockout mice express a *Cre* recombinase, which is flanked by YFP as reporter protein. Therefore, YFP was used to sort the $CD4^+Foxp3^+$ Treg and the $CD4^+Foxp3^-$ Treg cell population (Figure 8).

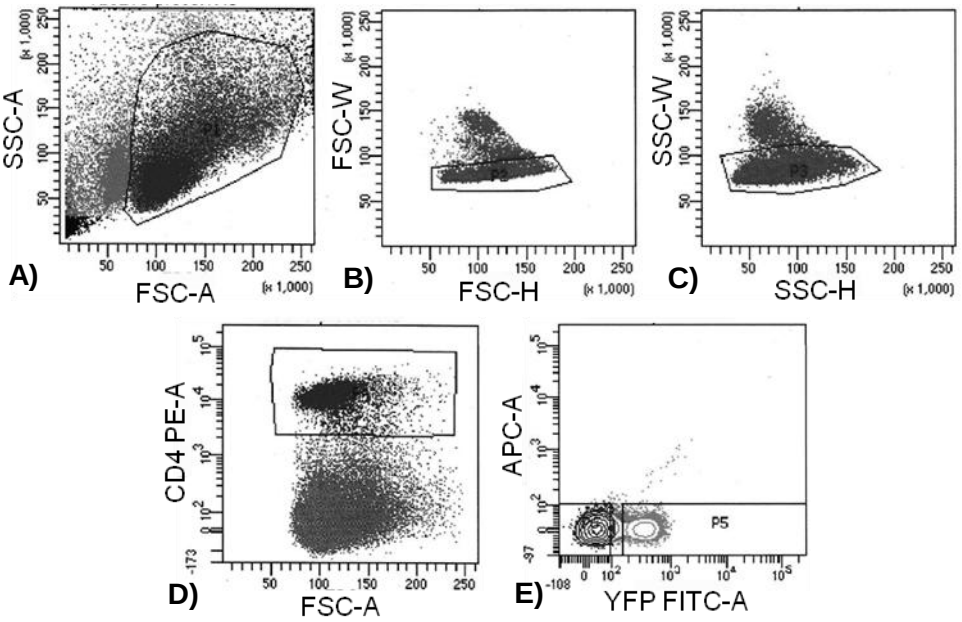

Figure 8: FACS gating strategy of splenocytes of a *Foxp3-Cre* mouse. (A) Scatter plot of the different cell types present in the cell suspension. **(B + C)** Gating used to select for single cells. **(D + E)** CD4 positive T cells were selected as CD4-PE positive cells (rectangular gate). The YFP signal was used to select for the Treg cells present in the CD4 positive T cell population. $CD4^+Foxp3^+$ T cells and thus Tregs were selected as YFP positive cells (cell population on the right). YFP negative cells were $CD4^+Foxp3^-$ T cells (cell population on the left). In a *Foxp3* specific GARP knockout (KO) mouse, YFP positive cells are Tregs not expressing GARP, while YFP negative cells are Tregs without *Cre* recombinase expression.

3. Injection of CD4$^+$ effector T and regulatory T cells into NOD scid gamma mice

The sorted splenocytes were injected via the tail vein of NSG (NOD *scid* gamma) mice at a concentration of $1.00 \cdot 10^6$ CD4$^+$ Th cells and $0.25 \cdot 10^6$ Treg cells in 200 µL PBS. NSG mice were housed in individually ventilated cages and sacrificed one week later.

4. Analysis of the homeostasis model

The NSG mice were sacrificed via cervical dislocation and the spleens were isolated. Two third of the spleens were used to make a single cell suspension as described before. Blood samples were also taken. Again, erythrocytes were lysed and cells were counted with the Hemavet 950FS.

4.1. Flow cytometry analysis on spleen tissue

Samples were prepared from each mouse to perform combined surface and intracellular staining for CD45, CD4 and Foxp3 antigens. For the surface staining, anti-mouse CD45 eFluor450 (eBioscience, clone 30-F11) and anti-mouse CD4-APC-H7 (Miltenyi Biotec, Leiden, The Netherlands, clone GK1.5) were used. The antibodies were incubated for 30 minutes at 4°C.

Following washing of the cells in PBS, the intracellular staining was performed to assess Foxp3 expression. Therefore, cells were permeabilized with 1 mL of the fixation/permeabilization working solution during 18 hours at 4°C (Foxp3 staining buffer set, eBioscience). After incubation, permeabilization buffer (1x) was added and cells were again centrifuged for five minutes at 400 g. This step was repeated, followed by removal of the supernatant and resuspension of the remaining volume after decanting. To avoid aspecific binding, FcR block (anti-mouse CD16/CD32, eBioscience, clone 93) was added and cells were incubated for 10 minutes on ice, followed by incubation with the anti-mouse/rat Foxp3 PerCP-Cyanine 5.5 Ab (eBioscience, clone FJK-16s) during one hour at 4°C. After the incubation period, 2 mL of the permeabilization buffer was added and samples were centrifuged at 400 g for five minutes. The permeabilization step was repeated, followed by resuspension of the cells with 200 µL of the flow cytometry staining buffer (0.2% paraformaldehyde and 154 mM NaCl). Samples were acquired with a FACSVerse flow cytometer and analyzed using FACSuite software (Figure 9).

4.2. Cell counting and flow cytometry analysis on blood samples

Via the retro-orbital plexus, blood was taken both on citrate (3.8%) and on 5 mM EDTA. EDTA blood samples were used to determine total cell numbers with the Hemavet 950FS. The citrated blood was used for the flow cytometry analysis. Therefore, anti-mouse CD4-APC-H7 and anti-mouse CD45 eFluor450 Abs were added and samples were incubated for 20 minutes at RT, followed by a three minute incubation period with erythrocyte lysis buffer.

Samples were centrifuged, fixated with the flow cytometry staining buffer and analyzed with the FACSVerse flow cytometer.

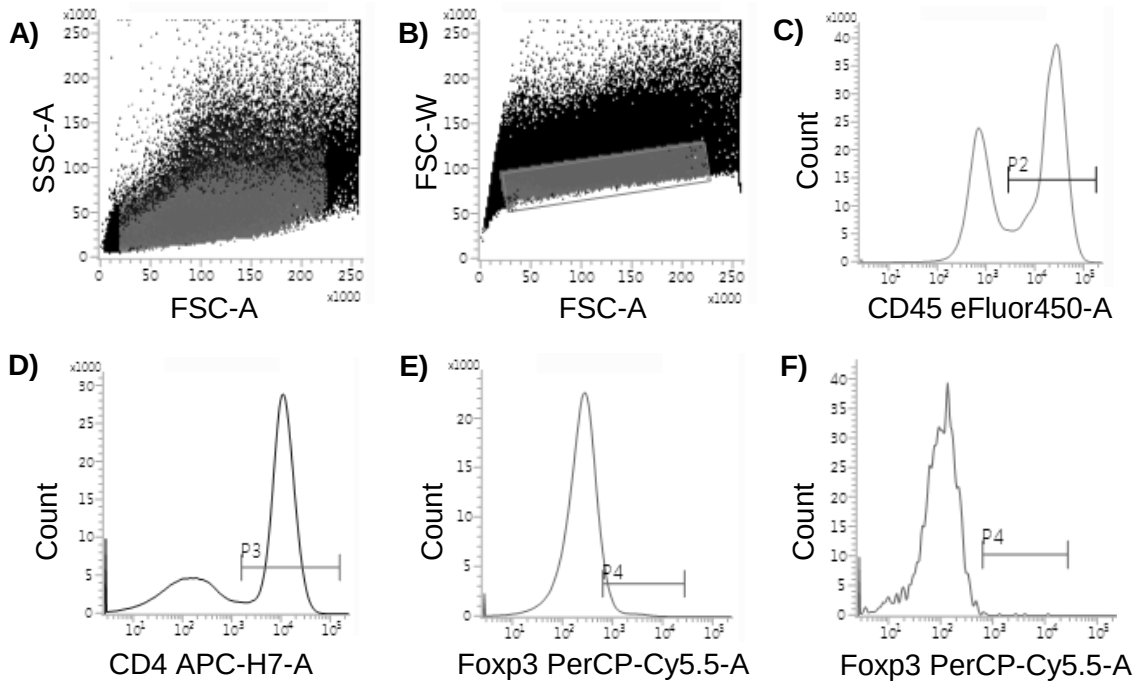

Figure 9: Gating strategy flow cytometry analysis of splenocytes isolated from a NSG mouse. (A) FS and SS show the scatter plot of the cell population present in the spleen. **(B)** Gating of the single cell population. **(C)** The gated cell population shows the CD45 positive cell population and thus the leukocytes (CD45 eFluor450, clone 30-F11). **(D)** The CD4 positive T cells were identified using a CD4 positive marker (CD4 APC-H7, clone GK1.5). **(E)** Foxp3 positive cells were detected with the anti-Foxp3 Ab (clone FJK-16s). **(F)** FMO (fluorescence minus one) of the anti-Foxp3 Ab.

4.3. Immunofluorescent staining on spleen tissue

One third of the spleen of the NSG mice was embedded in Tissue-Tek O.C.T Compound (Sakura Finetek Europe, Alphen aan den Rijn, The Netherlands), snap-frozen in liquid nitrogen and stored at -80°C. Cryosections were made of the spleen tissue with the Cryostat CM1950 (Leica Biosystems, Diegem, Belgium) (performed by Inge Pareyn) and used in an immunofluorescence assay. Briefly, cryosections were fixated for 15 minutes in acetone with a temperature of -20°C, followed by a five minutes washing step in PBS. Tissue was encircled with a DAKO Pen (Dako, Heverlee, Belgium) and blocked with PBS, 3% bovine serum albumin (BSA, Carl Roth GmbH + Co. KG, Karlsruhe, Germany) and 1% normal goat serum (NGS, Abcam, Cambridge, UK). After 30 minutes, the blocking solution was removed and anti-mouse CD4-PE was added (incubation for one hour at 37°C; 1/100 dilution in PBS, 3% BSA, 1% NGS). Subsequently, three washing steps with PBS were performed, followed

by an incubation of one hour in the dark with anti-rat IgG-PE (BioLegend, London, UK, clone Poly4054) at RT (1/100 dilution in PBS, 3% BSA, 1% NGS). Finally, cryosections were washed three times in PBS, three times in mQ water and mounted with the Prolong Gold antifade reagent that contains DAPI (Invitrogen).

Spleen sections were observed under the Eclipse TE-200 inverted fluorescence microscope (Nikon, Tokyo, Japan; 20x objective), which was coupled to a Hamamatsu CCD camera (ORCA-R2, Hamamatsu Photonics, Hamamatsu, Japan). Each section was illuminated with green excitation light (545-565 nm). Following excitation, each sample emitted red fluorescent light. The fluorescent images were analyzed with ImageJ (National Institutes of Health, MD) to determine the mean CD4 positive signal as a percentage of the total surface area.

Chapter 3 - The MCA tumor model

1. Induction of fibrosarcomas in regulatory T cell specific GARP knockout and littermate mice

Male Treg specific GARP knockout mice and their littermates were anaesthetized with 5% isoflurane in O_2 and their hind limbs were shaved. A suspension of MCA (Sigma Aldrich, St. Louis, Mo) in olive oil (4 mg/mL) was prepared and a dose of 100 µL was injected subcutaneously (s.c.) in the left hind limb. The right hind limb served as a control and received the same volume of olive oil only. The 25G needle stayed *in-situ* for 30 seconds to make sure that the MCA settled. Small leakages of the suspension were accounted as normal. Once a week, mice were checked for tumor development. The diameter of the hind limbs were measured with a digital caliper (Fine Science Tools GmbH, Heidelberg, Germany) and the difference between the legs was calculated and used to fit an exponential growth curve to estimate the growth rate *k* (mm/week, $Y = e^{kx}$ with *x* time in weeks and *Y* as the difference in diameter between the hind legs in mm). Once a tumor developed, tumor width, height and depth were measured to determine the tumor volume using the formula of an ellipsoid ($Volume = 4/3 \cdot \pi \cdot width \cdot height \cdot depth$), respectively. The number of weeks that a mice remained tumor-free was determined by calculating the standard deviation on the difference between the diameters of the hind legs until week nine. Differences in diameter exceeding this standard deviation were used to determine the tumor onset.

2. MCA tumor isolation and flow cytometry analysis

To determine the TILs present in the tumor, flow cytometry was performed on tumor tissue. Tumors were isolated, washed in PBS (Table 7) and cut into pieces to make a single cell suspension (see Chapter 2), which was diluted in 25 mL RPMI medium containing 10% fetal bovine serum (FBS) (all from Gibco, Life Technologies, Ghent, Belgium) and centrifuged at 400 g for six minutes.

Erythrocytes were lysed with 5 mL of the erythrocyte lysis buffer (Table 8) for 90 seconds at RT (previously described in Chapter 2). After centrifuging the cell suspension at 400 g for 10 minutes, cells were resuspended in PBS and counted with the Hemavet 950FS.

An equal amount of cells was put in four different tubes and centrifuged at 400 g for five minutes. After removal of the supernatant, cells were stained with anti-mouse CD45 eFluor450, anti-mouse CD3e-FITC (eBioscience, clone 145-2C11), anti-mouse CD4-APC-H7, anti-mouse GARP (LRRC32)-APC (Miltenyi Biotec, clone REA139) and anti-human REA control(I)-APC (Miltenyi Biotec, clone REA293). The antibodies were incubated at 4°C for 30 minutes. An intracellular Foxp3 staining was also performed as described (Chapter 1), but here the anti-mouse/rat Foxp3-PE Ab (eBioscience, clone FJK-16s) was used. Acquisition and analysis were performed with the FACSVerse and FACSuite software (Figure 10).

A GARP staining was also performed on cells of MCA tumors of littermate mice. The same protocol was applied as described above. The surface staining was performed with the anti-mouse CD45-FITC (ImmunoTools, GmbH, Friesoythe, Germany, clone IBL-5/25), the anti-mouse CD4-APC-Vio770 (Miltenyi Biotec, clone GK1.5), the anti-mouse GARP-PE (eBioscience, clone YGIC86) and the isotype control IgG2aκ-PE (BD, clone R35-95). The intracellular staining was performed with the anti-mouse Foxp3-PerCP-Cyanine5.5 Ab. Figure 11 shows the gating strategy acquired with the FACSVerse and FACSuite software.

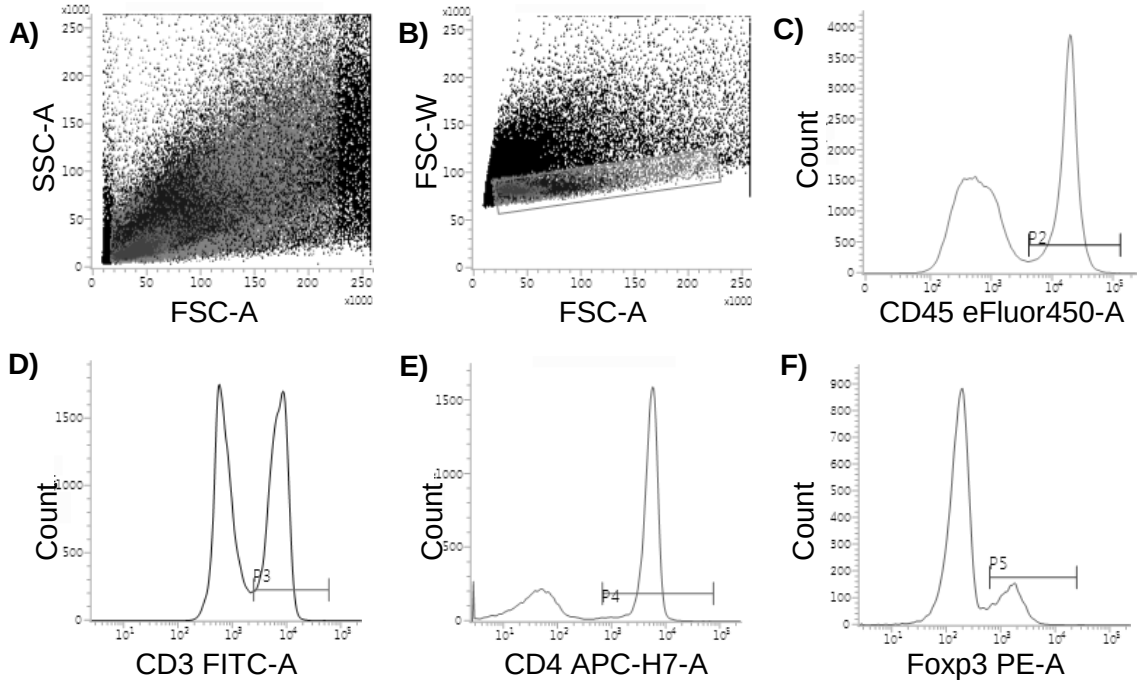

Figure 10: Gating strategy flow cytometry analysis of MCA-induced fibrosarcomas. Graphs represent the analysis of a *Foxp3* littermate (LM) mouse. **(A)** FS and SS show the scatter plot of the cell population present in the MCA tumor. **(B)** Gating of the single cells. **(C)** The gated cell population shows the CD45 positive cell population and thus the leukocytes (CD45 eFluor450, clone 30-F11). **(D)** The gated cell population is CD3 positive, which were T lymphocytes (CD3e-FITC, clone 145-2C11). **(E)** CD4 positive T cells were gated using the CD4-APC-H7 ab (clone GK1.5). **(F)** Gating of Foxp3 positive Tregs (clone FJK-16s).

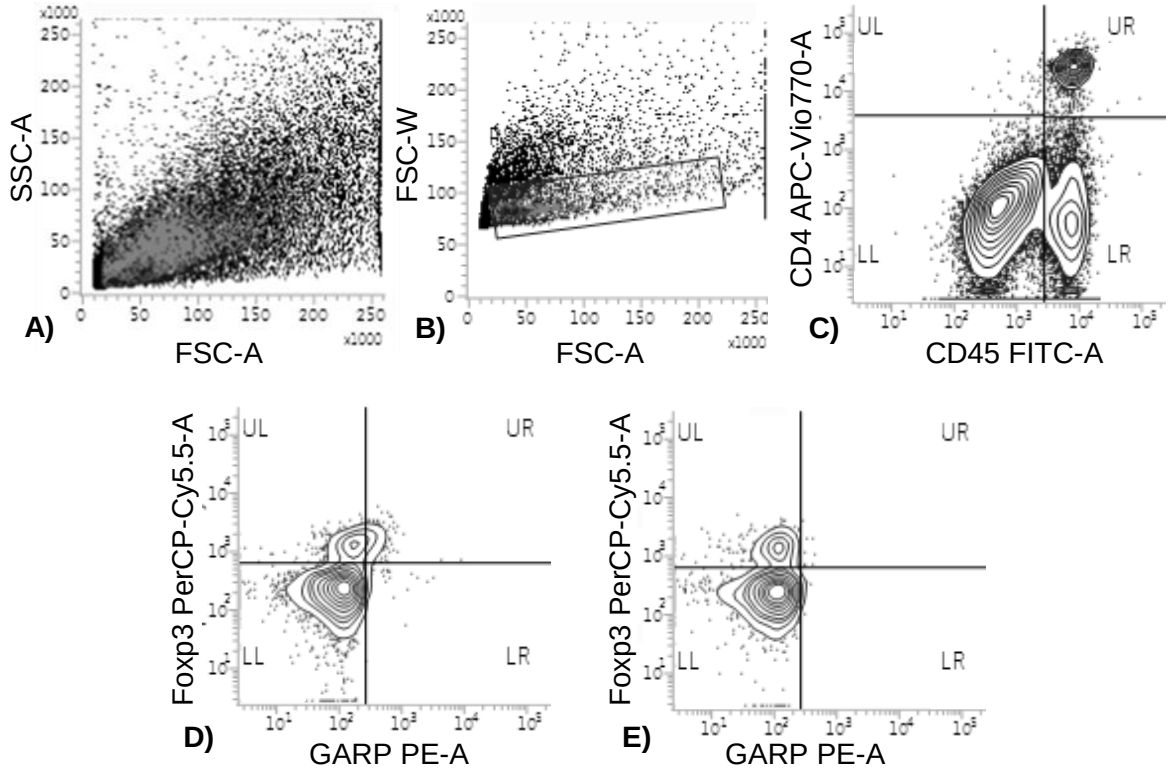

Figure 11: Gating strategy flow cytometry analysis for the presence of GARP on Tregs in MCA-induced tumors. (A) FS and SS show the scatter plot of the cell population in the single cell suspension of the MCA-induced tumor. **(B)** Gating of the single cells. **(C)** Scatter plot to gate the CD45 positive and CD4 positive cells (CD45-FITC, clone IBL-5/25; CD4-APC-Vio770, clone GK1.5). **(D)** Scatter plot to assess the Foxp3 positive and GARP positive cells (Foxp3-PerCP-Cy5.5, clone FJK-16s; GARP-PE, clone YGIC86), gated within CD4 positive T cells. **(E)** Isotype control of the GARP Ab (IgG2aκ-PE, clone R35-95).

Chapter 4 - The MC38 tumor model

1. Thawing of MC38 cell stocks

MC38 cells (kindly provided by Sophie Lucas, De Duve Institute, UCL, Brussels, Belgium) were thawed by putting the vial in a water bath of 37°C. Cells were brought into RPMI medium containing 10% FBS and 1% penicillin/streptomycin (Gibco, Life Technologies) with a temperature of 37°C and centrifuged at 1000 rpm for five minutes. The supernatant was removed and the pellet resuspended in RPMI medium. Cells were cultured in T-75 or T-125 culture flasks containing RPMI medium at 37°C and 5% CO_2.

2. MC38 cell passage

Cells were passed when 90% confluency was reached. Cells were collected and centrifuged at 1000 rpm for five minutes. Supernatant was decanted and the pellet was resuspended in RPMI medium. A split ratio of one flask in four was maintained.

3. Production of MC38 cell stocks

Harvested cells were centrifuged at 1000 rpm for five minutes and were resuspended in FBS and DMSO (dimethyl sulfoxide, ratio 10:1). Cell stock tubes contained 1 mL of the cell suspension and were frozen at -80°C before being stored in liquid nitrogen.

4. MC38 cell isolation and injection in endothelial specific GARP knockout and littermate mice

Harvested cells were counted with a Bürker chamber (Brand GmbH + Co. KG, Wertheim, Germany) and s.c. injected in the left flank of the endothelial specific GARP knockout and littermate mice at $5.00 \cdot 10^5$ cells in 200 µL PBS. Three times a week, tumor height and width were measured with a digital caliper. Mice were followed up for 40 days. When a tumor reached the predefined humane endpoint (volume of 1300 mm³), mice were sacrificed. Tumor volume was calculated with the following formula: $\text{Volume} = 4/3 \cdot \pi \cdot \text{width}^2 \cdot \text{height}$.

Chapter 5 - A wound healing and matrigel plug assay

1. Wound healing assay

1.1. Surgery

Endothelial specific GARP knockout and littermate mice were sedated with an intraperitoneal injection (100 µL/10 g body weight) of Ketamine (100 mg/mL) and Xylazine (20 mg/mL). The mice were shaved and Veet was applied to remove the fur. The mice were then taped on their ventral side on a heating pad and received pain relief injected s.c. in the flank (Vetergesic 0.3 mg/mL, 1/10 dilution, 100 µL s.c.). Using a 5 mm dermal biopsy punch (Stiefel Laboratories, Wavre, Belgium), a piece of skin was removed on the back of the mice. A silicone ring of 8 mm internal diameter was glued and stitched around the wound. The wound was moistened with 0.9% NaCl and covered with Tegaderm dressing. Every two days, a digital picture was taken of the wound, the Tegaderm was renewed and the wound was moistened with 0.9% NaCl. At day eight, mice were sedated with 5% isoflurane in O_2 and sacrificed by cervical dislocation. Wound dimensions were measured with ImageJ (National Institutes of Health, MD).

1.2. VWF-VIP staining on skin tissue sections

To determine vessel growth in the dorsal wounds, skin compromising the wound area was isolated at day eight and embedded in Tissue-Tek O.C.T Compound, snap-frozen in liquid nitrogen and stored at -80°C. Cryosections of the skin tissue were used for a von Willebrand Factor (VWF)-VIP staining.

Briefly, sections were fixated during 15 minutes in acetone with a temperature of -20°C, followed by a five minutes washing step in TBS (tris-buffered saline, Table 9) and 0.1% Tween20. Next, the sections were blocked for one hour with 10% normal swine serum (Jackson ImmunoResearch, St.-Martens-Latem, Belgium), 1% BSA and 0.1% Tween20. Sections were incubated overnight at 4°C with cross-reacting polyclonal rabbit anti-human VWF (Dako, 1/1500 dilution in TBS, 0.1% Tween20, 1% BSA). The following day, sections were washed three times for five minutes in TBS and 0.1% Tween20 and the endogenous peroxidase activity was blocked with 0.3% H_2O_2 (Sigma Aldrich) in TBS. After three washing steps, the sections were incubated for 30 minutes with anti-rabbit biotin (Dako, 1/500 dilution in TBS, 0.1% Tween20, 1% BSA), followed by 30 minutes incubation with the Vectastain ABC kit (Vector Laboratories, Brussels, Belgium). Sections were developed with the VIP HRP Substrate (Vector Laboratories) and washed in distilled H_2O and counterstained with methyl green at 60°C. Methyl green was washed away with distilled H_2O and sections were dehydrated by putting them in an ascending gradual series of respectively 50%, 70%, 95% and 100% ethanol and Sub-X. Finally, slides were dried and mounted with Sub-X mounting medium (Leica Biosystems). High-resolution digital images of the sections were made with the NanoZoomer-SQ (Hamamatsu Phototonics, Mont-Saint-Guibert, Belgium).

Table 9: Composition TBS buffer (pH 7.5, 5x).

Product	Supplier
1.50 M NaCl	Carl Roth GmbH + Co. KG, Karlsruhe, Germany
0.20 M Tris	Sigma Aldrich, St. Louis, Mo
dH_2O	-

2. Matrigel plug assay

2.1. Subcutaneous injection and isolation of the matrigel plug

The matrigel (Corning Matrigel basement membrane matrix growth factor reduced; Corning, NY) was thawed overnight at 4°C. A mixture of 500 µL matrigel, 300 ng/mL VEGF (R&D systems, 493-MV-005) and 700 ng/mL bFGF (basic fibroblast growth factor, R&D systems, 133-FB-025) was made. Endothelial specific GARP knockout and littermate mice were sedated with 5% isoflurane in O_2 and s.c. injected in the right groin. The needle remained *in-situ* for 30 seconds. After two weeks, mice were sacrificed and matrigels were recovered and embedded in Tissue-Tek O.C.T. Compound, snap-frozen in liquid nitrogen and stored at -80°C (s.c. injection and isolation of the matrigel plug were performed by drs. Elien Vermeersch).

2.2. VWF staining

Cryosections were made of the matrigel plug, followed by a VWF staining (performed by Inge Pareyn). A similar protocol was used as for the CD4 staining performed in Chapter 3 (4.4). Here, the blocking solution also contained TritonX100 (Table 10).

Table 10: Composition blocking solution VWF and CD31 staining.

VWF staining	CD31 staining	Supplier
PBS	PBS	See Table 7
3% BSA	1% BSA	Carl Roth GmbH + Co. KG, Karlsruhe, Germany
1% NGS	10% NGS	Abcam, Cambridge, UK
0.2% TritonX100		Sigma Aldrich, St. Louis, Mo;
	0.1% Tween20	Acros Organics, Geel, Belgium
Volume per slide	**200 µL**	

Anti-human VWF was used as the primary Ab and was applied for one hour at 37°C (1/1500 dilution in PBS, 0.2% TritonX100, 3% BSA, 1% NGS). The secondary Ab was anti-rabbit AF555 (Abcam, Cambridge, UK), which was incubated for one hour at RT (1/1000 dilution in PBS, 0.2% TritonX100, 3% BSA, 1% NGS).

2.3. CD31 staining

The cryosections of the matrigel plug were also used for a CD31 staining. Again, an identical protocol was used as for the CD4 and the VWF staining (Chapter 3 and Chapter 4). Here, washing steps were done in PBS and 0.1% Tween20 and a specific blocking solution was applied (Table 10). The primary anti-CD31 (Abcam, clone RM0031-1D12) was applied for one hour at 37°C (1/100 dilution in PBS, 0.1% Tween20, 3% BSA, 1% NGS). The secondary Ab anti-rat AF555 (Abcam) was applied for one hour at RT (1/1000 dilution in PBS, 0.1% Tween20, 3% BSA and 1% NGS).

2.4. Analysis of the matrigel plug sections

Matrigel plug sections were examined under the Eclipse TE-200 inverted fluorescence microscope (10x objective), which was coupled to a Hamamatsu CCD. Each section was illuminated with green excitation light (545-565 nm). Of each matrigel, sections were selected from the beginning, middle and end of the matrigel plug. Five pictures, with a total of 15 images of each matrigel plug, were taken of each section stained for VWF. Images taken at the center from sections stained with CD31 were not analyzed. Therefore, the analysis was performed on 12 images. To measure the VWF and CD31 positive signals as a percentage of the total surface, pictures were analyzed with ImageJ (National Institutes of Health, MD).

Chapter 6 - Statistics

Data were presented as mean ± standard deviation (SD). Two-way ANOVA with multiple comparisons and Bonferroni corrections was used to compare the tumor growth curves of the MCA and MC38 tumors. Statistical analysis of two independent groups was done by a two-tailed unpaired Student's *t*-test. To compare the mean of more than two independent groups, a one-way ANOVA analysis with multiple comparisons and Bonferroni corrections was performed. Analysis of more than two groups in combination with more than two independent variables was performed by a two-way ANOVA with multiple comparisons and Tukey posthoc tests. The Kaplan-Meier curves of the number of weeks mice remained tumor-free were compared using the Log-rank test. Association of genotype and tumor development was tested with the Fisher's Exact test to determine χ^2. Statistical analyses were performed with GraphPad Prism 6 (GraphPad Software, Inc., La Jolla, CA). Differences were considered significant at $p < 0.05$.

Part III: Results

Chapter 1 - Role of GARP on regulatory T cells in cancer

One objective of this thesis was to determine the role of GARP in the suppressive function of Tregs. Since GARP binds latent TGF-β, which is an important immunological regulator, we wanted to investigate whether there was a difference in suppressive capacity between Tregs with and without GARP. To study this, we performed the MCA tumor model in mice lacking GARP on Tregs and an *in vivo* Treg homeostasis model in NSG mice.

1. Genotyping of Foxp3 *mice*

To study the role of GARP on Tregs *in vivo*, Treg specific GARP knockout mice were generated. PCR was performed on gDNA of the mice to unravel their genotype. GARP expressed on Tregs is specifically knocked out when the *Cre* recombinase is present in combination with two *LoxP* sites flanking *Garp*. Littermate mice have only the two *LoxP* sites and do not express the *Cre* recombinase enzyme.

The presence of *LoxP* sites and *Cre* recombinase was determined and as shown in Figure 12A, *Garp* was homozygous floxed (181 bp) in all transgenic mice, since only one band was detected at 181 bp and not a combination of a band at 181 bp and 111 bp, which would represent heterozygous floxing of *Garp*. The presence of the *Cre-YFP* construct was identified by a second PCR and resulted in a fragment of 346 bp (Figure 12B).

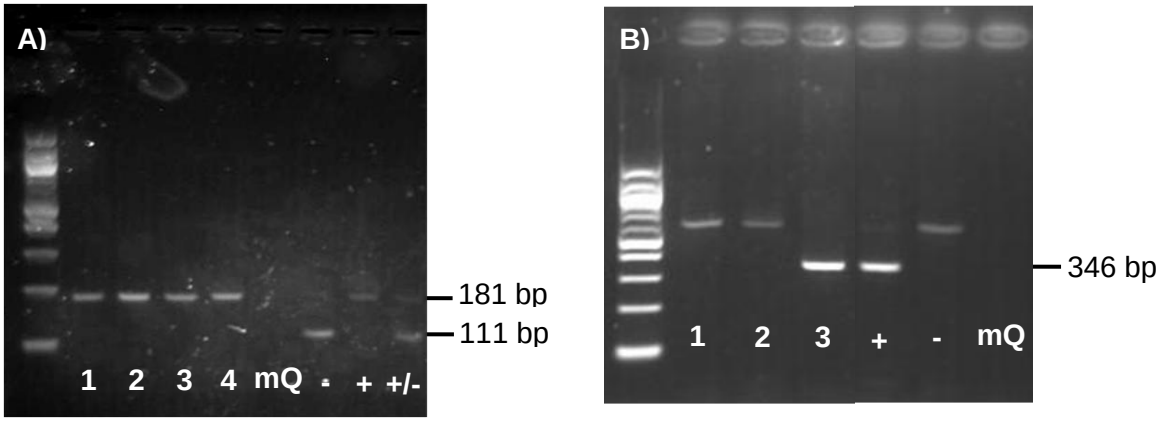

Figure 12: Genotypic analysis of gDNA from transgenic mice. (A) Determining the presence of *LoxP* sites. *LoxP* is measured at 181 bp and the WT allele (negative control) at 111 bp. Lanes 1 to 4 represent mice which are homozygous for *LoxP*. **(B) Determining the presence of *Cre* recombinase.** Presence of *Cre* is measured at 346 bp. Lane 3 is *Cre* positive. Lanes 1 and 2 represent mice that do not have the *Cre* gene. In each gel, positive (+) and negative (-) controls and mQ controls were included.

2. Mice lacking GARP on regulatory T cells are not resistant against MCA-induced fibrosarcomas

To investigate whether GARP expressed on Tregs, and as receptor for latent TGF-β, helps in shaping the tumor microenvironment and development, the Treg dependent MCA tumor

model was performed on Treg specific GARP knockout mice. A possible change in active TGF-β levels, caused by the Treg specific GARP knockout, could change the level and nature of invading immune cells into the tumor, which are necessary to destroy the cancer cells.

The MCA tumor model was performed in male *Foxp3* specific GARP knockout (n = 7) and littermate (n = 10) mice. Tumor growth was followed for a period of 29 weeks. Each week, the diameters of the hind legs were measured to determine the difference between the tumor and non-tumor leg, which was then used to establish the week of tumor onset and to calculate the tumor growth curve. Next to this, we analyzed each tumor to define the TILs present in the tumor.

2.1. MCA-induced fibrosarcoma incidence and growth kinetics in specific GARP knockout and littermate mice are not significantly different

Using flow cytometry, it was shown that 11 ± 3% of the Tregs present in the tumor of littermate mice express GARP.

By week 26, eight out of ten littermate mice and three out of seven knockout mice developed a tumor. A Kaplan-Meier curve was made of the weeks in which the mice were tumor-free to verify whether there was a difference in tumor onset. The Log-rank test shows that Treg specific GARP knockout mice did not have tumors at a significant later time point as compared to littermate mice (p = 0.1460, Figure 13A). To test whether tumor development was dependent of the genotype, the Fisher's Exact test was performed. This showed that the association between genotype (littermate or knockout) and tumor development was insignificant (p = 0.1600).

Mice were sacrificed 4 ± 2 weeks after the tumor had become detectable (Figure 13B). Figures 13C and 13D show that there was no difference in tumor growth in knockout and littermate mice, since the average tumor volume and growth rate k were not significantly different. The k value was 0.58 ± 0.27 mm/week in knockout and 0.76 ± 0.45 mm/week in littermate mice.

In conclusion, no significant difference was seen in tumor onset and tumor growth kinetics when comparing Treg specific GARP knockout and littermate mice.

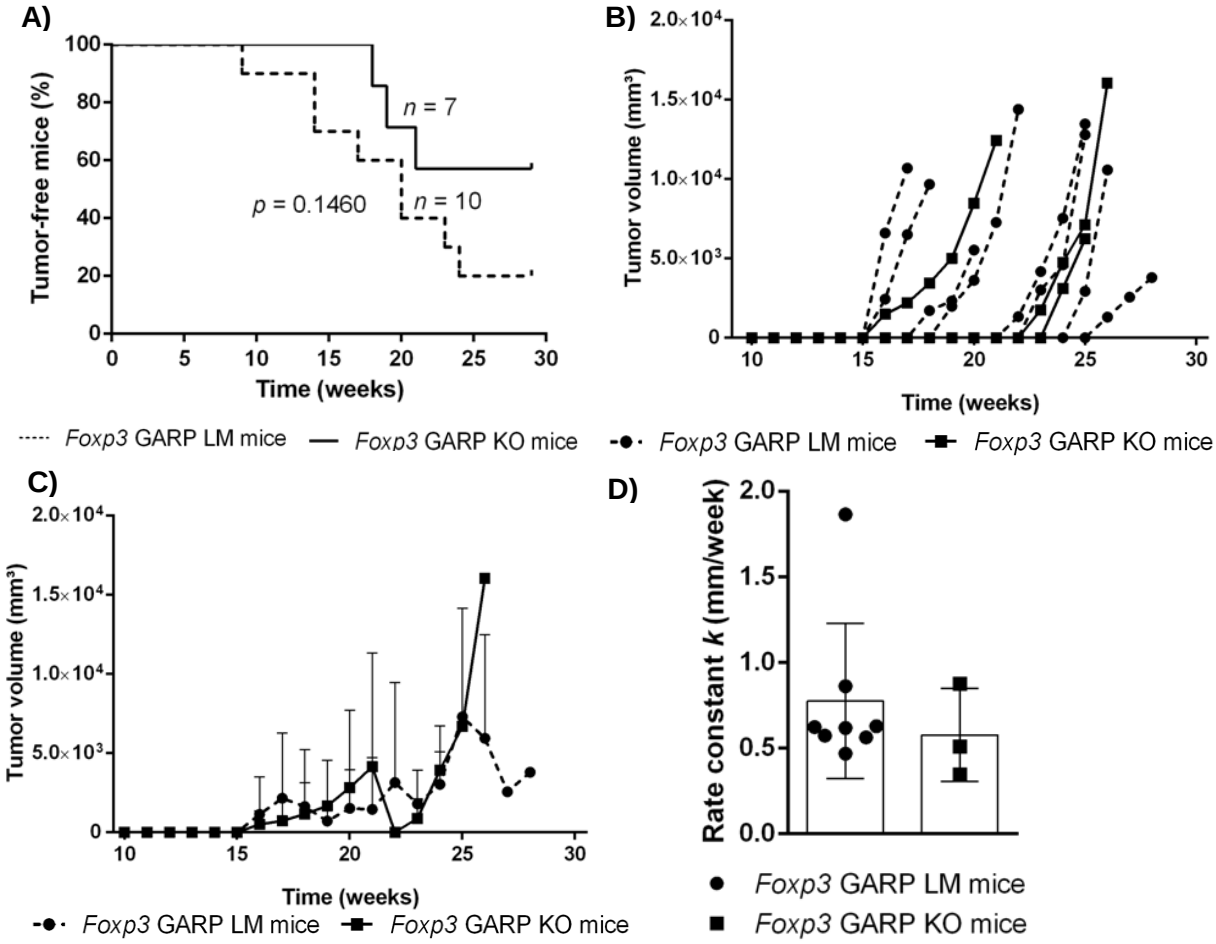

Figure 13: Onset and growth kinetics of MCA-induced tumors in Treg specific GARP knockout and littermate mice. (A) A Kaplan-Meier curve of the number of weeks a mouse remained tumor-free was made to determine whether LM mice develop a tumor at an earlier point in time as compared to the Treg specific GARP KO mice. Data were analyzed with the Log-rank test. **(B)** For each mouse (KO: *n* = 3; LM: *n* = 8), tumor volume (mm³) was calculated based on tumor width, height and depth. **(C)** The mean tumor volume (mm³) of KO (*n* = 3) and LM (*n* = 8) mice. Data show mean tumor volume ± SD and were analyzed with a two-way ANOVA with Bonferroni corrections. **(D)** The rate constant *k* (mm/week) of each exponential growth curve was determined. Data show mean *k* ± SD and were analyzed with an unpaired Student's *t*-test.

2.2. Tumor infiltrating lymphocytes in the fibrosarcomas are not significantly different in regulatory T cell specific GARP knockout and littermate mice

To investigate if GARP on Tregs is involved in the infiltration of immune cells in the MCA tumor, a predefined set of immune cell types was measured in the tumor. In the single cell suspension of the tumor, $CD45^+$ cells (leukocytes) were measured to determine the percentage of $CD3^+$ cells (T lymphocytes) and $CD4^+$ Th cells, while the $Treg^+$ percentage was determined in the $CD4^+$ cell population.

This showed that the percentages of the $CD3^+$ cells, $CD4^+$ Th cells and Tregs were not significantly different in tumors of Treg specific GARP knockout and littermate mice (Figure 14A). Tumor volumes were used to calculate the absolute cell number/mm³ for each tumor. Again, no difference in immune cell population was seen between the tumors of Treg specific knockout and littermate mice (Figure 14B).

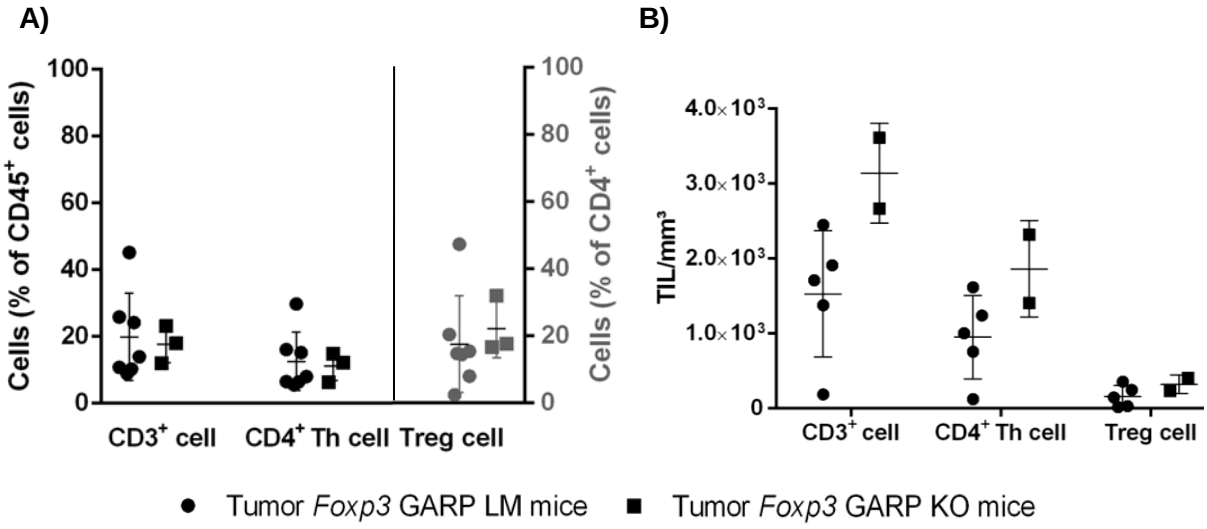

Figure 14: Relative and absolute abundance of TILs in MCA-induced tumors. (A) $CD3^+$, $CD4^+$ and $Treg^+$ cell percentages measured in the flow cytometry analysis of the MCA-induced tumors of LM (*n* = 7) and KO (*n* = 3) mice. Data show mean cell percentages ± SD and were analyzed with two-way ANOVA with multiple comparisons and Bonferroni corrections. **(B)** Using the cell percentages and the cell numbers of the Hemavet analysis, the absolute cell number was calculated, which was then divided by the tumor volume to gain the absolute cell number per mm³. Data show mean ± SD (LM: *n* = 5; KO: *n* = 2).

3. GARP deficient regulatory T cells show no compromised suppressive capacity

The results of the MCA tumor model and the TILs did not show a significant difference between Treg specific GARP knockout and littermate mice. However, the tumor microenvironment is complex. Therefore, we opted for an *in vivo* homeostasis model to determine the difference between Tregs expressing and not expressing GARP in a tumor-free setting.

Splenocytes of *Foxp3-Cre* mice were sorted and this resulted in $5.50 \cdot 10^6$ $CD4^+$ Th cells and $1.00 \cdot 10^6$ wild-type Tregs. Sorting of splenocytes of *Foxp3* specific GARP knockout mice resulted in $7.00 \cdot 10^6$ $CD4^+$ Th cells and $1.00 \cdot 10^6$ Tregs lacking GARP. The cells were injected in three groups of NSG mice. The first group was injected with $CD4^+$ Th cells and it was expected that $CD4^+$ Th cells without Tregs would proliferate without regulation. The second group received a combination of wild-type Tregs and $CD4^+$ Th cells, in which the

Tregs were supposed to control the proliferation of the $CD4^+$ Th cells. Since the third group of mice was injected with a combination of $CD4^+$ Th cells and Tregs lacking GARP, it was hypothesized that the Tregs would be less suppressive resulting in more proliferation of the $CD4^+$ Th cells. However, since Tregs also have other suppressive mechanisms, such as cell-surface molecules and inhibitory cytokines, it was expected that $CD4^+$ Th cells would proliferate less as compared to the first group.

One week after injection of the cells in the NSG mice, blood samples were taken and spleens were isolated to determine the absolute $CD4^+$ Th and Tregs cell numbers (Figure 15). In the spleen, absolute cell numbers show that the $CD4^+$ Th cells injected in combination with Tregs expressing GARP have significantly less proliferative capacity as compared to $CD4^+$ Th cells that were injected alone ($p < 0.001$; Figure 15A). The significant difference in $CD4^+$ Th cell numbers was not found in the blood samples (Figure 15B).

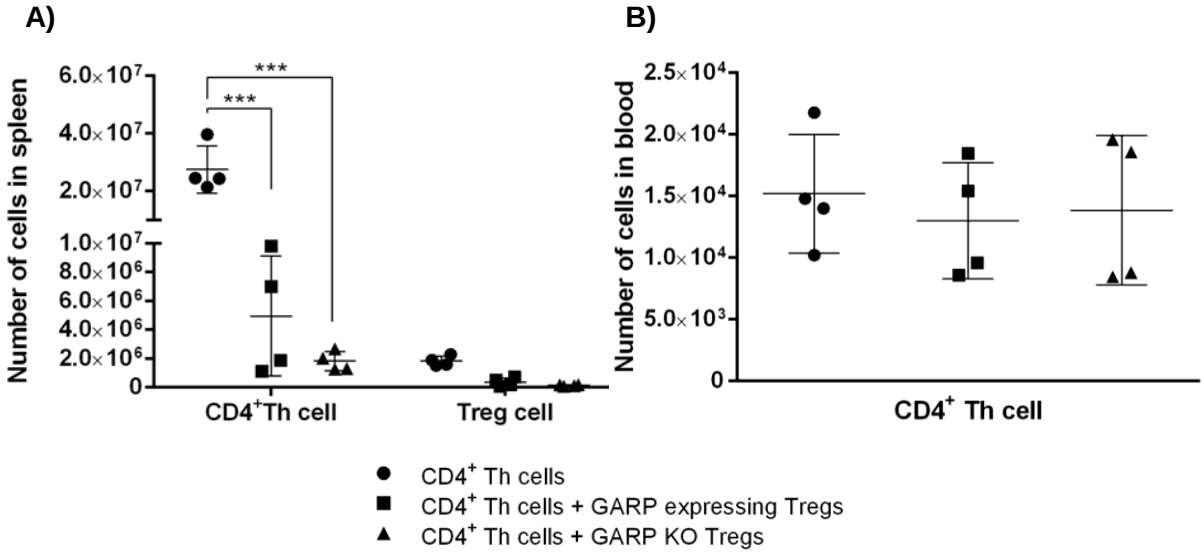

Figure 15: Absolute cell numbers of $CD4^+$ Th cells and Tregs (A) in spleen and (B) in blood of NSG mice injected with $CD4^+$ Th cells and/or Tregs. (A) Absolute cell numbers of the $CD4^+$ Th and Treg cell populations in the spleen were calculated with the cell percentages acquired from the flow cytometry analysis and with the cell numbers from the Hemavet analysis. **(B)** Absolute cell numbers in the blood (V = 130 µL) were calculated with the cell percentages from the flow cytometry analysis and with the cell numbers from the Hemavet analysis with EDTA blood. Data show mean cell numbers ± SD and was analyzed with one-way ANOVA with multiple comparisons and Tukey posthoc tests. Each group consists of $n = 4$. Asterisks show significant differences (*** $p < 0.001$).

When comparing the $CD4^+$ Th cell numbers in the spleens of mice injected with $CD4^+$ Th cells alone or with a combination of $CD4^+$ Th cells and Tregs not expressing GARP, a significant difference was also found in that $CD4^+$ Th cell numbers were significantly lower in

mice injected with $CD4^+$ Th cells and Tregs knockout for GARP as compared to the group that received only $CD4^+$ Th cells ($p < 0.001$; Figure 15A).

No difference was found between the second and third group, which were injected with wild-type Tregs and Tregs not expressing GARP, since absolute $CD4^+$ Th cell numbers in the spleen did not show a significant difference (Figure 15A). These results were in parallel with the absolute $CD4^+$ Th cell numbers in the blood, in which again no difference was found (Figure 15B).

Besides $CD4^+$ Th cells, we also looked at Treg cell numbers. This showed that Tregs were present in the spleens of the three groups of injected mice and that there were no significant differences in absolute Treg cell numbers (Figure 15A).

The results of the MCA model and the *in vivo* homeostasis model suggest that GARP expressed on Tregs does not contribute to the suppressive activity of Tregs in the regulation of the $CD4^+$ Th cell population.

To confirm the flow cytometry results of the $CD4^+$ Th cell numbers present in the spleen, an immunofluorescent staining was performed on spleen sections (Figure 16). The mean CD4 positive signal revealed no significant difference between the mice receiving only $CD4^+$ Th cells and the mice receiving a combination of $CD4^+$ Th cells and Tregs expressing GARP. In contrast, $CD4^+$ Th cell numbers in mice injected with $CD4^+$ Th cells were significantly higher when compared to the cell numbers of mice treated with $CD4^+$ Th cells and Tregs lacking GARP ($p < 0.05$). Hence, these results oppose the hypothesis and the flow cytometry analysis.

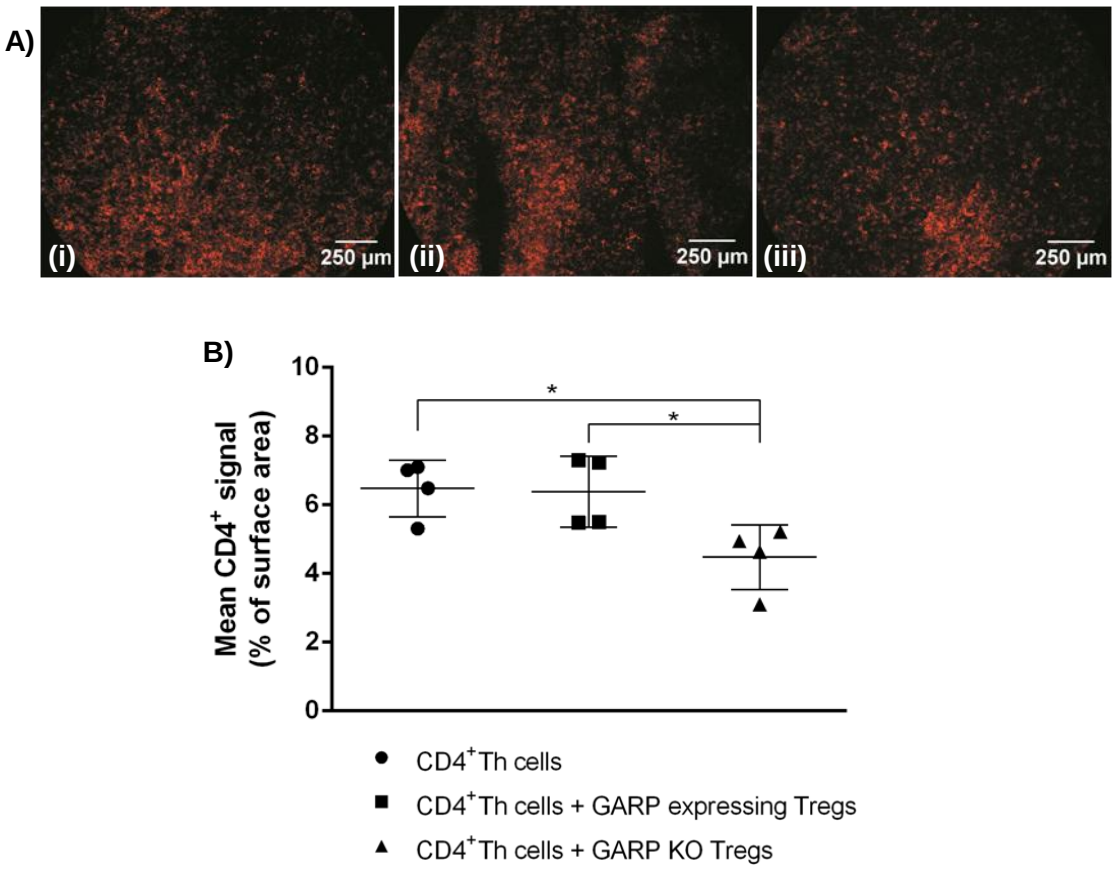

Figure 16: Immunofluorescence microscopy on spleens isolated from NSG mice injected with $CD4^+$ Th cells and/or Tregs. (A) Fluorescence images (20x magnification) of the CD4 staining of spleen sections of mice receiving $CD4^+$ Th cells (i), $CD4^+$ Th cells and Tregs expressing GARP (ii) and $CD4^+$ Th cells and Tregs knockout for GARP (iii). $CD4^+$ Th cells were stained with anti-mouse CD4-PE (clone GK1.5). The secondary antibody was anti-rat IgG-PE (clone Poly4054). **(B)** Five pictures were taken and analyzed by two individuals who were blinded to avoid bias. Data were pooled and show mean CD4 positive signal ± SD and were analyzed with a one-way ANOVA with multiple comparisons and Tukey posthoc tests. Asterisks show significant differences (* $p < 0.05$).

Chapter 2 - Role of GARP on endothelial cells in cancer

Next to the role of GARP on Tregs, we also wanted to determine the role of endothelial GARP in cancer, since Carambia *et al.* reported that the LSECs of the liver, which express GARP on their cell surface, induce naïve T cells to become Tregs in a TGF-β dependent manner (Carambia *et al.*, 2014). Besides this, Hahn *et al*. reported that sGARP also has a regulatory impact on the $CD4^+$ Th cell population (Hahn *et al*., 2013, 2016). Hence, it might be possible that endothelial GARP also contributes to immune regulation and thus to the promotion of tumor development.

1. Genotyping of Tie2 *mice*

To study the role of endothelial GARP in cancer, we first needed to genotype *Tie2* specific GARP knockout mice. The same PCR protocol was used as for genotyping the *LoxP* sites in the *Foxp3* specific GARP knockout and littermate mice.

The presence of the *Cre* recombinase identifies the mouse as a knockout. The DNA fragment of *Cre* is at 450 bp (Figure 17). A DNA fragment of 230 bp is also present. This DNA is derived from internal control primers. Littermate mice only show a band at 230 bp.

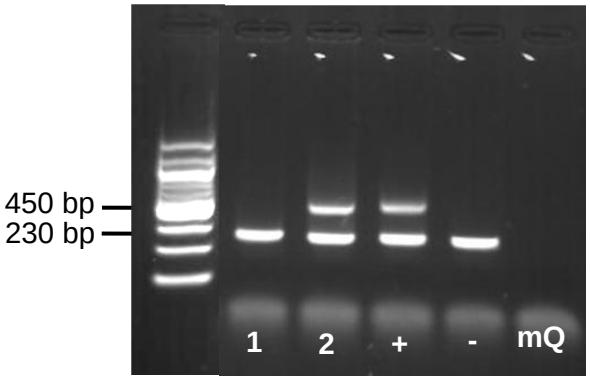

Figure 17: Genotypic analysis of gDNA from transgenic mice. Presence of *Cre* is measured at 450 bp. Lane 2 is *Cre* positive. Lane 1 does not have the *Cre* gene. Positive (+), negative (-) controls are included together with mQ. Positive control is derived from a mouse with known expression of *Cre*, while the negative control was from a C57BL6 mouse not expressing *Cre*.

2. Specific GARP knockout mice develop significant smaller MC38 tumors when compared to littermate mice

MC38 cells were s.c. injected into the flank of endothelial specific GARP knockout (n = 5) and littermate (n = 7) mice. Figure 18 shows the evolution of the tumors throughout the experiment. Tumors started to develop two to seven days post-injection.

The tumor volumes of littermate mice can be divided into three phases. In the first phase, tumors increased until day 14, on which tumors had a mean volume of 325.82 ± 158.05 mm^3. During the second phase, from day 14 until day 21, tumors decreased again to 262.94 ±

199.64 mm³. The last phase was characterized by tumor growth until the end of the experiment on day 40. Tumors had a final mean volume of 804.24 ± 692.12 mm³. Two of the seven littermate mice were able to reject the tumor on days 14 and 19, respectively.

A similar first stage was also observed in knockout mice, since tumors continued to grow until day 16 and reached a mean volume of 254.49 ± 120.14 mm³. However, the second phase was not characterized by tumor growth, but by a decrease in volume. Two out of five knockout mice also rejected their tumor on day 16. Three and five days later, on days 19 and 21, two other mice had undetectable tumors. So, in total, four out of five EC specific GARP knockout mice were able to reject the tumor. Only one knockout mouse could not. The tumor volume of that mouse remained steady-state until day 35 and was then followed by an increase in volume.

On day 33, a significant difference in the mean tumor volume was found between endothelial specific GARP knockout and littermate mice ($p < 0.05$) when the average tumor volume in knockout mice was 57.61 ± 109.42 mm³ and in littermate mice 557.85 ± 449.24 mm³. This significant difference remained until the end of the experiment. Therefore, these results show that endothelial specific GARP knockout mice were significantly better protected against the development of MC38 tumors when compared to littermate mice.

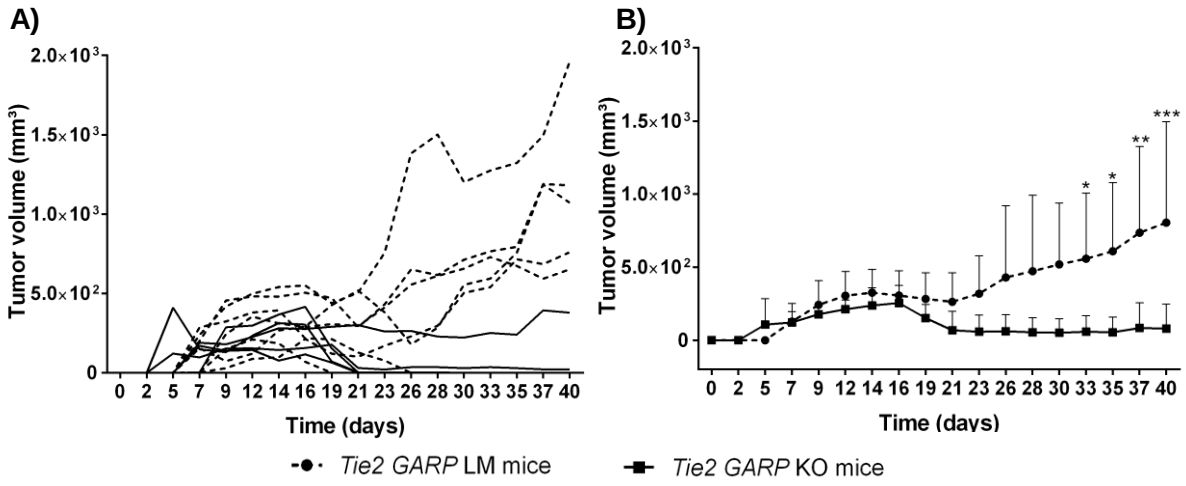

Figure 18: Development of MC38 tumors in endothelial specific GARP knockout and littermate mice. A) Individual graphs of tumor volumes of endothelial specific GARP KO (n = 5) and LM (n = 7) mice. **B)** Data represent mean tumor volumes ± SD. Significant differences are shown with asterisks: * $p < 0.05$, ** $p < 0.01$, *** $p < 0.001$. Data were analyzed with two-way ANOVA with multiple comparisons and Bonferroni correction.

Chapter 3 - Role of GARP on endothelial cells in angiogenesis

In situations, such as wound repair and angiogenesis, a temporarily shortage in TGF-β might occur. ECs might represent important storage sites that are able to compensate for the higher demand of TGF-β. To address this, different *in vivo* assays were performed, such as a wound healing and matrigel plug assay in endothelial specific GARP knockout mice and littermate mice.

1. Endothelial specific GARP knockout mice do not show a difference in blood vessel formation in the matrigel plug when compared to littermate mice

The matrigel plug assay is a known model to study angiogenesis. VEGF and bFGF present in the matrigel plug will recruit ECs, which form blood vessels in the matrigel plug. To test whether endothelial GARP plays a role in the formation of vasculature, matrigel sections were analyzed by measuring VWF and CD31. Both are markers for the detection of ECs.

Fluorescent images illustrate that both VWF and CD31 were present throughout the matrigel plug sections (Figure 19). However, the observed CD31 signal was higher at the edges of the sections when compared to the center of most of the sections, while the VWF signal was detected at both the edges and the center. Also, the CD31 signal was more continuous when compared to the VWF signal.

After analysis of the microscope images, it was seen that matrigel plugs formed in littermate and knockout mice were not significantly different in fluorescent VWF and CD31 signals and thus in blood vessel density (Figure 19).

2. Endothelial specific GARP knockout mice do not show a difference in wound healing when compared to littermate mice

Another method to study angiogenesis in a more physiological and *in vivo* context is via a wound healing model. The skin on the back of endothelial specific GARP knockout mice and littermates was surgically removed and regrowth of the skin was measured.

In Figure 20, the dorsal wounds of endothelial specific GARP knockout and littermate mice were compared. Wound size gradually declined in littermate mice from 100 ± 24% on day zero to 32 ± 15% on day eight, compared to a decrease of 100 ± 19% on day zero to 26 ± 12% on day eight for knockout mice respectively. Thus, no significant difference was found on any of the days in the eight day follow-up period between knockout and littermate mice.

Besides the measurement of wound closure, blood vessels were also detected in the wound area of both knockout and littermate mice by using a staining for VWF (Figure 21). Healthy skin that was not injured during the wound healing assay was identified by the presence of hair follicles. In newly formed skin, hair follicles were not yet present.

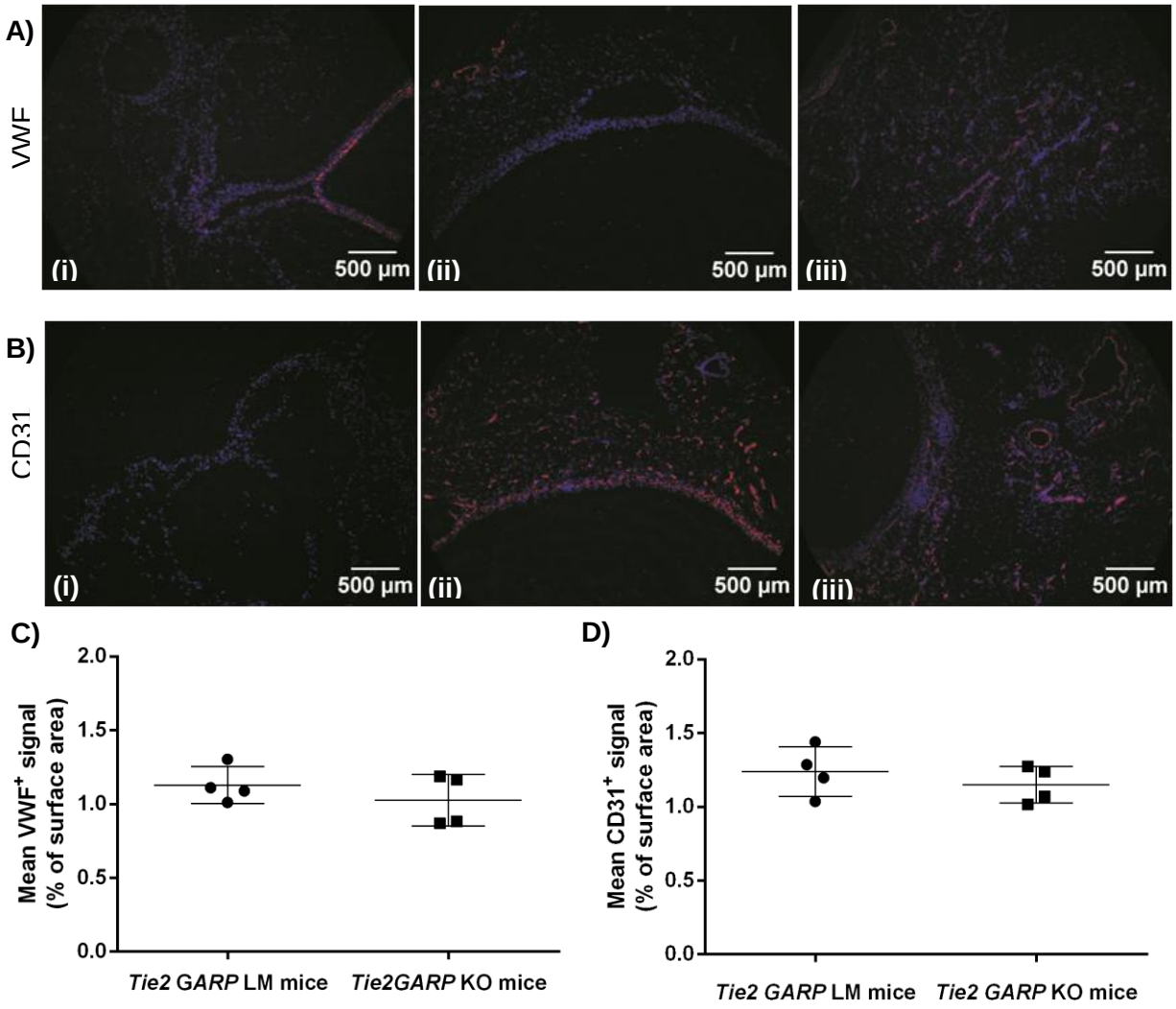

Figure 19: Immunofluorescence staining on matrigel plugs of endothelial GARP specific knockout and littermate mice. (A+B) Fluorescent VWF (A) and CD31 (B) staining and analysis on cryosections of the center (i) and the edges (ii, iii) of a matrigel plug of a endothelial GARP specific KO mouse. **A)** Sections were stained with the primary anti-human VWF Ab and anti-rabbit AF555 as secondary Ab. **B)** Sections were stained with the anti-CD31 Ab and the secondary Ab anti-rabbit AF555. DNA was stained with DAPI (blue). Both CD31 and VWF emit a red fluorescent signal. **(C)** Analysis of five images of sections stained with VWF. **(D)** Analysis of four images of sections stained with CD31. Data show mean fluorescent signal ± SD and were analyzed with an unpaired Student's *t*-test.

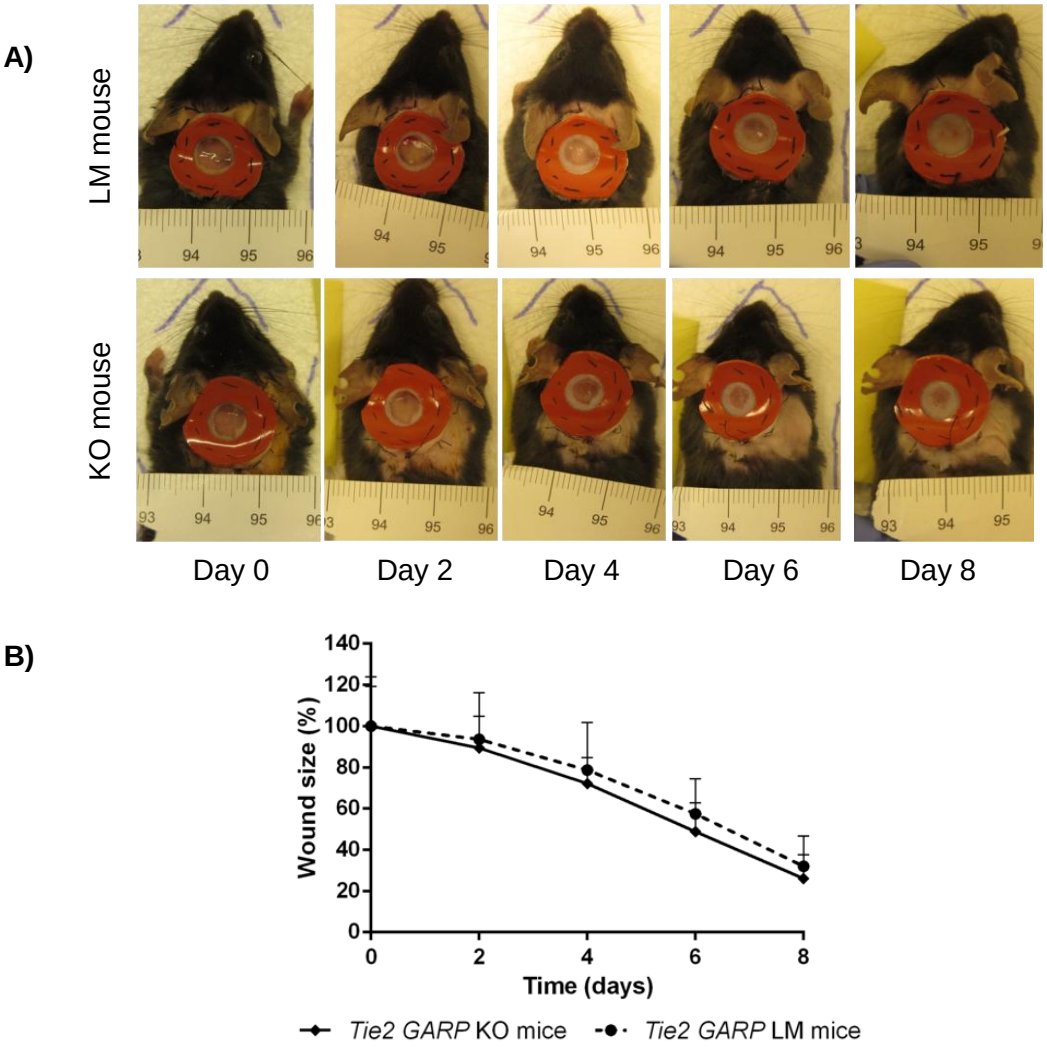

Figure 20: Wound size (%) of dorsal wounds in endothelial specific GARP knockout and littermate mice. (A) Pictures of dorsal wounds in endothelial specific GARP KO and LM mice. Pictures were taken every other day in a period of eight days. **(B)** Wound size was calculated as the surface area relative to the surface area to the silicone ring. Mean surface areas of day zero were considered as 100% in order to compare wound sizes between mice and days. Specific GARP KO mice (*n* = 7) were compared to LM mice (*n* = 7). Data represent mean wound size ± SD and were analyzed with two-way ANOVA with multiple comparisons and Bonferroni correction.

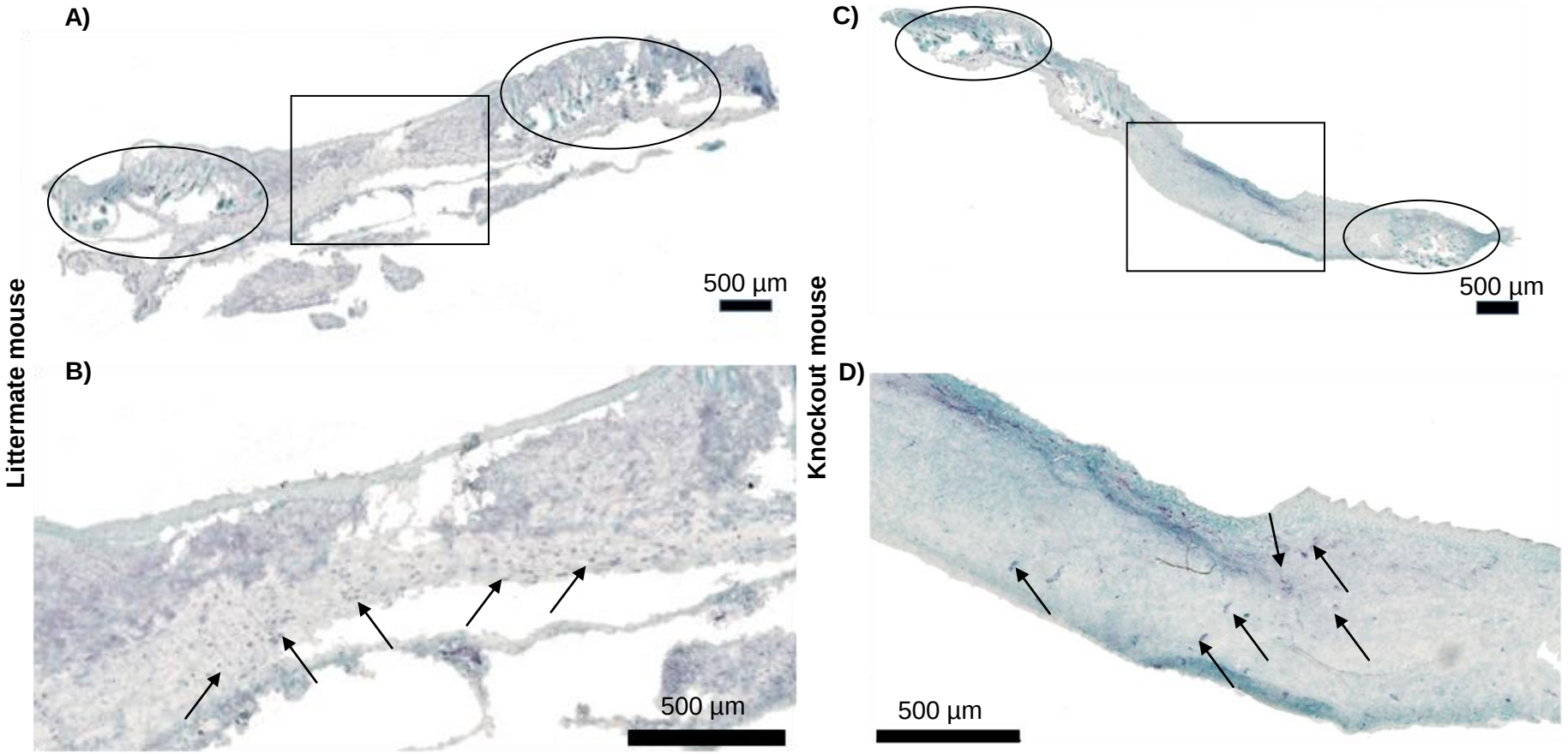

Figure 21: Immunohistochemistry on newly formed skin tissue in the dorsal wounds of endothelial specific GARP knockout and littermate mice. **(A)** Skin section of a LM mouse stained with anti-human VWF and VIP HRP substrate. VWF positive cells are purple, DNA was stained with methyl green (magnification 1.25x). Hair follicles are found in the ovals. **(B)** Detail of the wound area from (A) (magnification 5x, rectangle). Arrows indicate the newly formed vessels. **(C)** Skin section of a KO mouse stained with anti-human VWF and VIP HRP substrate (magnification 1.25x). Hair follicles are located in the ovals. **(D)** Detail of the wound area from (C) (magnification 5x). Arrows indicate the newly formed vessels.

Part IV: Discussion & conclusions

TGF-β is an important cytokine regulating several processes in the body. Amongst other functions, it has a key role in maintaining the delicate balance between immunity and immunological tolerance. In this perspective, inhibition of it can lead to the development of autoimmune diseases. Next to this, mutations in the TGF-β pathway can induce cancer or defective angiogenesis. Interestingly, latent TGF-β is bound to GARP that is expressed on Tregs and ECs, cell types that are involved in development of certain tumors and angiogenesis, respectively. Hence, we wanted to investigate the role of GARP on Tregs and ECs in the development of cancer and the formation of blood vessels.

Tregs use, next to soluble and membrane-bound factors, TGF-β in order to regulate and suppress autoreactive $CD4^+$ T cells. To test the role of GARP expressed on Tregs in these inhibitory activities, we set up the MCA model and induced fibrosarcomas in the hind legs of Treg specific GARP knockout and littermate mice. In some cancers, it is known that Tregs are attracted to the tumor microenvironment and start to secrete TGF-β in order to inhibit other immune cells. We expected that, due to a possible difference in TGF-β levels, tumor onset and/or development would be impacted in knockout as compared to littermate mice.

Betts *et al.* reported that 70 to 80% of the MCA-injected mice had a fibrosarcoma by week 29 (Betts *et al.*, 2007). In line with these findings, 80% of littermate mice in our hands developed a tumor by week 27. In contrast, only 40% of the MCA treated Treg specific GARP knockout mice had a tumor 27 weeks post-injection.

The first tumor of a littermate mouse was seen in the 10th week of the experiment, which is in parallel with the reported 12 weeks after MCA injection (Betts *et al.*, 2007). The first tumor in a knockout mouse was detected in week 18 of the experiment. This suggested that tumors in knockout mice developed later as compared to littermate mice. However, the Kaplan-Meier curve, which determined the number of weeks a mice remained tumor-free, was not able to confirm this observation, since the difference was insignificant. Next to this, no significant difference was found in the tumor growth rate *k* between tumors of knockout and littermate mice.

These results do not confirm our hypothesis that tumors in knockout mice would develop differently. However, the experiment has not yet come to an end and mice will be followed for another 20 weeks. In those weeks, other tumors may develop in both littermate and knockout mice, although we think that we have reached the top-level of tumor development in littermate mice, since already 80% have a tumor.

Next to determining tumor incidence and onset, we also identified the TILs present in the tumor to examine if a difference in tumor immune response could be detected between tumors of littermate and Treg specific GARP knockout mice. It was already shown that MCA tumors are infiltrated by Tregs (Betts *et al.*, 2007; Hindley *et al.*, 2011).

We could confirm Treg infiltration in the tumors of both knockout and littermate mice, but to a lower extent when compared to the study of Betts. They reported Treg percentages present in the $CD4^+$ T cell population in the tumor between 40% and 50%, while we see much lower Treg levels present in the $CD4^+$ cell population, ranging from 19 ± 15% in littermate mice to 22 ± 8% in knockout mice.

We are currently not able to explain this discrepancy in cell percentages between our results and the data from Betts and Hindley. Including more mice in new experiments could give more clarity, since we were only able to report on the TILs in the tumors of three Treg specific GARP knockout mice. This results in difficulties when comparing littermate and knockout mice and thus in making solid conclusions about immune cell infiltration.

Also, our hypothesis stated that the lack of GARP on Tregs would cause a drop in TGF-β levels in the tumor microenvironment. We did not look into that during this thesis, but it might be a good idea to try to find out whether this is indeed the case in Treg specific GARP knockout mice. Measuring levels of active TGF-β could be done by measuring the phosphorylation level of the Smad transcription factors, which are phosphorylated after binding of active TGF-β to its receptor (Stockis *et al*., 2009a).

The puzzling data obtained from the MCA model led us to the direct assessment of the suppressive capacities of Tregs expressing GARP and Tregs not expressing GARP in an *in vivo* homeostasis model performed in NSG mice. The model would tell us, without the complexity of tumors, whether a difference can be observed between the two types of Tregs.

Results showed a significant increase of absolute $CD4^+$ Th cells in mice injected with only $CD4^+$ Th cells when compared to mice receiving a combination of Tregs and $CD4^+$ Th cells. These results clearly show the effect of the presence of Tregs on the proliferative capacity of the $CD4^+$ Th cells.

In parallel with the MCA tumor model, we did not find a change in the suppressive capacity of the two types of Tregs in the cell numbers retrieved from the spleen. $CD4^+$ Th cells did not differ in knockout and littermate mice. Treg numbers were also similar, which means that the absence of GARP has no influence on the functionality of the Tregs and that Tregs are able to suppress the $CD4^+$ Th cell population independently of GARP.

We also tried to confirm the flow cytometry analysis of the spleen by performing an immunofluorescence assay on spleen sections, but we were unable to reproduce the flow cytometry results. This might be attributed to the analysis of the fluorescent images. Flow cytometry is more sensitive as compared to immunofluorescent staining, since single cells are detected.

Our data from the *in vivo* homeostasis model are in parallel with previous assays performed *in vitro* on T effector proliferation with Tregs lacking GARP and wild-type Tregs. Both types of Tregs were equally suppressive (Edwards *et al*., 2013). It was shown, in another *in vivo* homeostasis model, that Tregs are dependent on TGF-β, but that they do not have to secrete it themselves in order to be suppressive (Fahlén *et al*., 2005). Therefore, it might be possible in our model that Tregs expressing and not expressing GARP do not use TGF-β bound to GARP in order to suppress.

The *in vitro* study of Edwards *et al.* also showed that Tregs without GARP were no longer able to induce the differentiation from $CD4^+$ Th cells into Tregs (Edwards *et al*., 2013). Considering the Treg population of our *in vivo* model, an equal number of Tregs in the spleen was found in the three groups of mice. This probably reflects that, *in vivo,* Tregs without GARP were still able to regulate the differentiation of $CD4^+$ Th cells into Tregs, as could the wild-type Tregs. We also detected Tregs in mice injected with $CD4^+$ Th cells only. These Tregs were probably induced from $CD4^+$ Th cells without TGF-β derived from Tregs. They reached cell numbers that were as high as in the mice injected with Tregs. However, these induced Tregs were not able to suppress the proliferation of the $CD4^+$ Th cells. An explanation is lacking, but the time needed for the differentiation of Tregs might be too long to stop the proliferation of the injected $CD4^+$ Th cells.

We also tested the role of GARP on ECs in cancer. Carambia *et al*. reported the expression of GARP on liver LSECs, which contributed to the differentiation of peripheral T cells into induced Tregs via TGF-β released from the GARP/LAP complex (Carambia *et al.*, 2014). Next to this, sGARP derived from Tregs was shown to have immunoregulatory functions on naïve $CD4^+$ T cells independent from Tregs (Hahn *et al*., 2013, 2016). Hence, GARP might also be shed from the EC surface and exhibit suppressive functions.

Little is known about endothelial GARP in cancer development and therefore, a hypothesis was formulated in accordance to the data of Carambia *et al*. and Hahn *et al*. Since TGF-β bound to GARP might induce Tregs, we wanted to know whether the development of tumors, in which it is established that Tregs are involved, differ in endothelial specific GARP knockout mice compared to littermate mice. Loss of GARP, and thus a possible reduction in bioactive TGF-β, could lead to less Tregs or Tregs that are less suppressive. To test this, we challenged endothelial specific GARP knockout and littermate mice with the MC38 tumor cell line.

Overt tumors were detected in both knockout and littermate mice, which increased in volume during the first sixteen days of the experiment. Two out of seven littermate mice and four out of five knockout mice rejected the tumor. Tumors of the other littermate mice increased in

volume until the end of the experiment. This eventually resulted in a significant difference in tumor volumes between knockout and littermate mice from day 33 onwards.

These interesting results could be explained in two ways. A first answer is already stated in our hypothesis. A lower level of active TGF-β, due to loss of GARP as receptor for latent TGF-β, can lead to less differentiation from $CD4^+$ Th cells into Tregs and thus to a drop in the suppressive actions of Tregs on the immune cells that are attacking the cancer cells. Whether this is true is so far unknown, but recent research performed in platelet specific GARP knockout mice could shine a light on our hypothesis. Rachidi *et al.* have recently shown that significantly more platelet specific GARP knockout mice were able to reject MC38 tumors when compared to wild-type mice. Tumors in wild-type mice increased in volume, because GARP mediated the activation of TGF-β. This caused, through the GARP/TGF-β complex, suppression of the antitumor immunity. Absence of GARP resulted in significantly lower levels of active TGF-β and thus in effective antitumor immunity. On top of these results, knockout mice had less Tregs in their tumors (Rachidi *et al*., 2017).

The results of the platelet specific GARP knockout mice might possibly be applicable to explain the rejection of tumors in endothelial specific GARP knockout mice. However, we have not yet evidence that this is true and it will be noteworthy to also check this in our experimental setting by measuring TGF-β levels and the number of Tregs.

A second possibility might that, because of the endothelial specific GARP knockout and thus a possible drop in TGF-β levels, blood vessels are malformed. It is already known that TGF-β is not only involved in immunity, but also in blood vessel formation through VEGF and that mice deficient in TGF-β show several defects (Ferrari *et al*., 2009). In general, we do not think that the loss of the endothelial GARP/TGF-β complex induces severe problems. In addition, since all mice developed first stage tumors, and tumors need newly formed blood vessels when they reach a volume of more than two cubic millimeters (Nishida *et al.*, 2006), we do not think that a problem with blood vessel formation is the cause of the difference between knockout and littermate mice. Arguments contributing to this conclusion on the MC38 model come from the wound healing and matrigel plug assays that we performed in this study. Both assays did not reveal significant differences between endothelial specific GARP knockout and littermate mice.

However, we need to be careful in drawing conclusions from these assays. First of all, only a small number of mice was included. Consequently, statistical power was low.

Second, we have some concerns regarding the matrigel plug assay. Although it is the method of choice for the *in vivo* analysis of angiogenesis, we encountered some difficulties. Matrigel plugs show high heterogeneity in volume. Despite injecting the same volume, plugs vary greatly in the three dimensional plane. This might lead to great variability in the analysis

and can only be overcome by using averaged data of different sections of the same matrigel plug. Next to immunofluorescent staining, it might be interesting to use reverse transcription-quantitative PCR to quantitatively evaluate the amount of endothelium formed in the matrigel plug. This might avoid the variability between the matrigel plugs and provide a more accurate quantification (Coltrini *et al.*, 2013).

Finally, we used both a VWF and a CD31 staining to visualize the blood vessels. Sections stained with VWF mostly showed signal in the center and at the edges, while the sections stained with CD31 often had no signal at the center. Therefore, five VWF images were analyzed per mouse as compared to four of the CD31 staining. Although this did not result in a difference in mean fluorescent signal when comparing both markers in the assay, CD31 is known as the better marker, since VWF is not a specific EC marker. It is also present in platelets. Next to this, presence of VWF in blood vessels depends on the type of organ and the type of blood vessel (Randi *et al.*, 2013; Yuan *et al.*, 2016).

These models show that endothelial GARP is not involved in angiogenesis. Other models should be used in the future to confirm this conclusion. Examples could be studying the blood vessel formation in the postnatal retina or in mouse ears, since the ear and eye are highly vascularized. An advantage of such assays is that mice would not need to be manipulated as in the above described assays (Stahl *et al.*, 2010; Starke *et al*., 2011).

Three major conclusions can be drawn from this study. First, no significant difference in tumor onset and incidence was found between Treg specific GARP knockout and littermate mice. This might be explained by the functionality of the Tregs, since Tregs lacking GARP were as suppressive when compared to wild-type Tregs: no differences were found in TILs present in the MCA-induced tumors or in the $CD4^+$ Th cell numbers in mice injected with a combination of $CD4^+$ Th cells and Tregs that did or did not express GARP in the *in vivo* homeostasis model (Figures 22A, 22B). Second, results from the MC38 model indicate that endothelial GARP seems to have an influence on cancer development, as significantly more endothelial specific GARP knockout mice were able to reject subcutaneous tumors, while most of the littermates could not (Figures 22C, 22D). There is no doubt that these date are highly promising. That is why the experiments will be repeated and elaborated more thoroughly in order to unravel the underlying mechanism. Finally, blood vessel formation was not defective in endothelial specific GARP knockout mice as shown in our preliminary experiments.

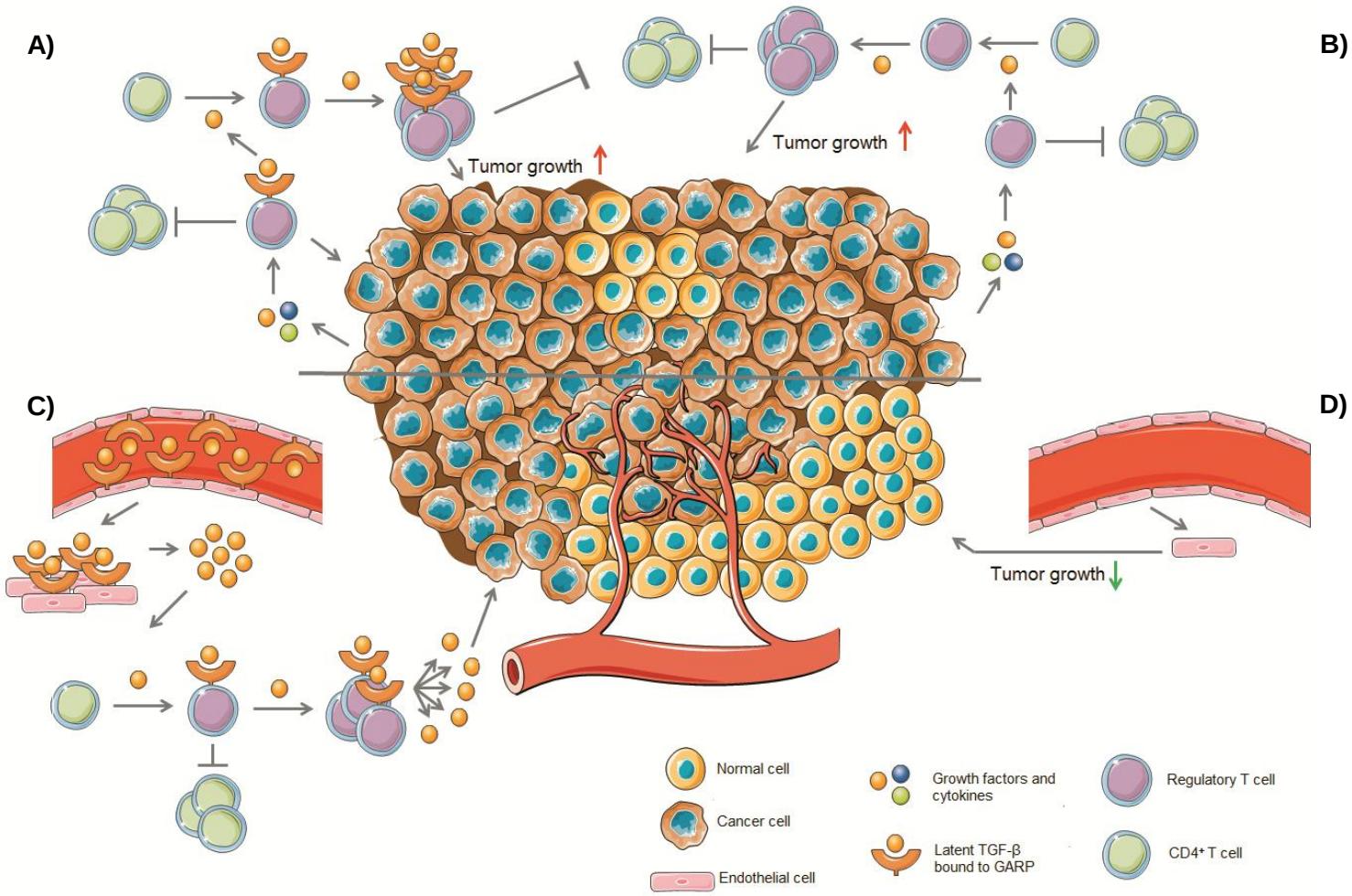

Figure 22: GARP on regulatory T (A, B) and endothelial cells (C, D) in cancer. (A, B) Tregs expressing GARP (A) and Tregs not expressing GARP (B) are not different in their suppression of $CD4^+$ T effector cells. No difference was found in TILs between MCA tumors isolated from Treg specific GARP KO and LM mice. Also, tumor onset and growth kinetics were not significantly different. **(C, D)** Mice expressing GARP (C) on ECs had significantly bigger tumors, when compared to endothelial specific KO mice (D).

References

Andrews, R. K., Gardiner, E. E., Shen, Y., Whisstock, J. C., & Berndt, M. C. (2003). Glycoprotein Ib-IX-V. *Int J Biochem Cell Biol*, *35*(8), 1170-1174.

Bekri, S., Adélaïde, J., Merscher, S., Grosgeorge, J., Caroli-Bosc, F., Perucca-Lostanlen, D., Kelley, P. M., Pébusque, M. J., Theillet, C., Birnbaum, D, & Gaudray, P. (1997). Detailed map of a region commonly amplified at 11q13-->q14 in human breast carcinoma. *Cytogenet Cell Genet*, 79, 125–131.

Betts, G., Twohig, J., Van den Broek, M., Sierro, S., Godkin, A., & Gallimore, A. (2007). The impact of regulatory T cells on carcinogen-induced sarcogenesis. *Brit J Cancer*, *96*(12), 1849–1854.

Budhu, S., Wolchok, J., & Merghoub, T. (2014). The importance of animal models tumor immunity and immunotherapy. *Curr Opin Genet Dev*, *24*(1), 46-51.

Burnet, S. M. (1957). Cancer - A biological approach. *Brit Med J*, *1*, 841–847.

Carambia, A., Freund, B., Schwinge, D., Heine, M., Laschtowitz, A., Huber, S., Wraith, D. C., Korn, T., Schramm, C., Lohse, A. W., *et al*. (2014). TGF-β-dependent induction of CD4+CD25+Foxp3+ Tregs by liver sinusoidal endothelial cells. *J Hepatol*, *61*(3), 594–599.

Carmeliet, P., & Jain, R. K. (2011). Molecular mechanisms and clinical applications of angiogenesis. *Nature*, *473*(7347), 298–307.

Carrillo-Galvez, A. B., Cobo, M., Cuevas-Ocaña, S., Gutiérrez-Guerrero, A., Sánchez-Gilabert, A., Bongarzone, P., García-Pérez, A., Muñoz, P., Benabdellah, K., Toscano, M. G., *et al*. (2015). Mesenchymal stromal cells express GARP/LRRC32 on their surface: Effects on their biology and immunomodulatory capacity. *Stem Cells*, *33*(1), 183–195.

Chen, T., Carter, D., Garrigue-Antar, L., & Reiss, M. (1998). Transforming growth factor beta type I receptor kinase mutant associated with metastatic breast cancer. *Cancer Res*, *58(*21), 4805–4810.

Coltrini, D., Di Salle, E., Ronca, R., Belleri, M., Testini, C., & Presta, M. (2013). Matrigel plug assay: evaluation of the angiogenic response by reverse transcription-quantitative PCR. *Angiogenesis*, *16*(2), 469-477.

Cuende, J., Lienart, S., Dedobbeleer, O., van der Woning, B., De Boeck, G., Stockis, J., Huygens, C., Colau, D., Somja, J., Delvenne, P., *et al*. (2015). Monoclonal antibodies against GARP/TGF- 1 complexes inhibit the immunosuppressive activity of human regulatory T cells in vivo. *Sci Transl Med*, *7*(284), 284ra56.

Curiel, T. J., Coukos, G., Zou, L., Alvarez, X., Cheng, P., Mottram, P., Evdemon-Hogan, M., Conejo-Garcia, J. R., Zhang, L., Burrow, M., *et al*. (2004). Specific recruitment of regulatory T cells in ovarian carcinoma fosters immune privilege and predicts reduced survival. *Nat Med*, *10*(9), 942–949.

Datto, M. B., Li, Y., Panus, J. F., Howe, D. J., Xiong, Y., & Wang, X. F. (1995). Transforming growth factor beta induces the cyclin-dependent kinase inhibitor p21 through a p53-independent mechanism. *PNAS*, *92*(12), 5545–5549.

DeRycke, M., Charbonneau, B., Preston, C., Kalli, K. R., Knutson, K. L., Rider, D. N., and Goode, E. L. (2013). Towards understanding the genetics of regulatory T cells in ovarian cancer. *Oncoimmunology*, *2*(6), e2435.

Dunn, G. P., Old, L. J., & Schreiber, R. D. (2004). The three Es of cancer immunoediting. *Annu Rev Immunol*, 22, 329–360.

Edwards, J. P., Fujii, H., Zhou, A. X., Creemers, J., Unutmaz, D., & Shevach, E. M. (2013). Regulation of the expression of GARP/latent TGF-β1 complexes on mouse T cells and their role in regulatory T cell and Th17 differentiation. *J Immunol*, *190*(11), 5506-5515.

Edwards, J. P., Thornton, A. M., & Shevach, E. M. (2014). Release of active TGF-β1 from the latent TGF-β1/GARP complex on regulatory T cells is mediated by integrin β8. *J Immunol*, *193*(6), 2843-2849.

Eming, S. A., Brachvogel, B., Odorisio, T., & Koch, M. (2007). Regulation of angiogenesis: Wound healing as a model. *Prog Histochem Cyto*, *42*(3), 115–170.

Facciabene, A., Peng, X., Hagemann, I. S., Balint, K., Barchetti, A., Wang, L.-P., Gimotty, P. A., Gilks, C. B., Lal, P, Zhang, L, & Coukos, G. (2011). Tumor hypoxia promotes tolerance and angiogenesis via CCL28 and Treg cells. *Nature*, *475*(7355), 226–230.

Fahlén, L., Read, S., Gorelik, L., Hurst, S. D., Coffman, R. L., Flavel, R. A., & Powrie, F. (2005). T cells that cannot respond to TGF-beta escape control by CD4+CD25+ regulatory T cells. *J Exp Med*, *201*(5), 737-746.

Ferrari, G., Pintucci, G., Seghezzi, G., Hyman, K., Galloway, A. C., & Mignatti, P. (2006). VEGF, a prosurvival factor, acts in concert with TGF-β1 to induce endothelial cell apoptosis. *PNAS*, *103*(46), 17260–17265.

Ferrari, G., Cook, B. D., Terushkin, V., Pintucci, G., & Mignatti, P. (2009). Transforming growth factor-beta 1 (TGF-β1) induces angiogenesis through vascular endothelial growth factor (VEGF)-mediated apoptosis. *J Cell Physiol*, *219*(2), 449–458.

Ferrari, G., Terushkin, V., Wolff, M. J., Zhang, X., Valacca, C., Poggio, P., Pintucci, G., & Mignatti, P. (2012). TGF-β1 Induces Endothelial Cell Apoptosis by Shifting VEGF Activation of $p38^{MAPK}$ from the Prosurvival p38β to Proapoptotic p38α. *Mol Cancer Res, 10*(5), 605–614.

Fleming, N. I., Jorissen, R. N., Mouradov, D., Christie, M., Sakthianandeswaren, A., Palmieri, M., Day, F., Li, S., Tsui, C., Lipton, L., *et al.* (2013). SMAD2, SMAD3 and SMAD4 mutations in colorectal cancer. *Cancer Res*, *73*(2), 725–735.

Francisco, L. M., Salinas, V. H., Brown, K. E., Vanguri, V. K., Freeman, G. J., Kuchroo, V. K., & Sharpe, A. H. (2009). PD-L1 regulates the development, maintenance, and function of induced regulatory T cells. *J Exp Med*, *206*(13), 3015–3029.

Francisco, L. M., Sage, P. T., & Sharpe, A. H. (2010). The PD-1 pathway in tolerance and autoimmunity. *Immunol Rev*, *236*, 219-242.

Freeman, G. J., Long, A. J., Iwai, Y., Bourque, K., Chernova, T., Nishimura, H., Fitz, L. J., Malenkovich, N., Okazaki, T., Byrne, M. C., *et al*. (2000). Engagement of the PD-1 immunoinhibitory receptor by a novel B7 family member leads to negative regulation of lymphocyte activation. *J Exp Med*, *192*(7), 1027–1034.

Friedline, R. H., Brown, D. S., Nguyen, H., Kornfeld, H., Lee, J., Zhang, Y., Appleby, M., Der, S. D., Kang, J., & Chambers, C. A. (2009). CD4+ regulatory T cells require CTLA-4 for the maintenance of systemic tolerance. *J Exp Med*, *206*(2), 421–34.

Garín, M. I., Chu, N. C., Golshayan, D., Cernuda-Morollón, E., Wait, R., & Lechler, R. I. (2007). Galectin-1: A key effector of regulation mediated by CD4+CD25+ T cells. *Blood*, *109*(5), 2058–2065.

Gauthy, E., Cuende, J., Stockis, J., Huygens, C., Lethé, B., Bommer, G., Coulie, P. G., & Lucas, S. (2013). GARP Is Regulated by miRNAs and Controls Latent TGF-β1 Production by Human Regulatory T Cells. *PLoS ONE*, *8*(9), e76186.

Gerhardt, H., Golding, M., Fruttiger, M., Ruhrberg, C., Lundkvist, A., Abramsson, A., Jeltsch, M., Mitchell, C., Alitalo, K., Shima, D., & Betsholtz, C. (2003). VEGF guides angiogenic sprouting utilizing endothelial tip cell filopodia. *J Cell Biol*, *161*(6), 1163–1177.

Girardi, M., Oppenheim, D. E., Steele, C. R., Lewis, J. M., Glusac, E., Filler, R., Hobby, P., Sutton, B., Tigelaar, R. E., & Hayday, A. C. (2001). Regulation of cutaneous malignancy by gammadelta T cells. *Science*, *294*(5542), 605–609.

Gondek, D. C., Lu, L.-F., Quezada, S. A., Sakaguchi, S., & Noelle, R. J. (2005). Cutting edge: Contact-mediated suppression by CD4+CD25+ regulatory cells involves a granzyme B-dependent, perforin-Independent mechanism. *J Immunol*, *174*(4), 1783–1786.

Grady, W. M., Myeroff, L. L., Swinler, S. E., Rajput, A., Thiagalingam, S., Lutterbaugh, J. D., Neumann, A., Brattain, M. G., Chang, J., Kim, S. J., *et al.* (1999). Mutational inactivation of transforming growth factor beta receptor type II in microsatellite stable colon cancers. *Cancer Res*, *59*(2), 320–324.

Grossman, W. J., Verbsky, J. W., Barchet, W., Colonna, M., Atkinson, J. P., & Ley, T. J. (2004). Human T regulatory cells can use the perforin pathway to cause autologous target cell death. *Immunity*, *21*(4), 589–601.

Guillot, N., Kollins, D., Gilbert, V., Xavier, S., Chen, J., Gentle, M., Reddy, A., Bottinger, E., Jiang, R., Rastaldi, M. P., *et al.* (2012). BAMBI regulates angiogenesis and endothelial homeostasis through modulation of alternative TGFβ signaling. *PLoS ONE*, *7*(6), e39406.

Hahn, S. A., Stahl, H. F., Becker, C., Correll, A., Schneider, F. J., Tuettenberg, A., & Jonuleit, H. (2013). Soluble GARP has potent antiinflammatory and immunomodulatory impact on human CD4+ T cells. *Blood*, *122*(7), 1182-1191.

Hahn, S. A., Neuhoff, J., Landsberg, J., Schupp, J., Eberts, D., Leukel, P., Bros, M., Weilbaecher, M., Grabbe, S., Tueting, T., *et al*. (2016). *Oncotarget*, *7*(28), 42996-43009.

Herbert, S. P., & Stainier, D. Y. (2011). Molecular control of endothelial cell behaviour during blood vessel morphogenesis. *Nat Rev Mol Cell Biol*, *12*(9), 551–564.

Hindley, J. P., Ferreira, C., Jones, E., Lauder, S. N., Ladell, K., Wynn, K. K., Betts, G. J., Singh, Y., Price, D. A., Godkin, A. J, *et al.* (2011). Analysis of the T cell repertoires of tumor-infiltrating conventional and regulatory T cells reveals no evidence for conversion in carcinogen-induced tumors. *Cancer Res*, *71*(3), 736-746.

Izumoto, S., Arita, N., Ohnishi, T., Hiraga, S., Taki, T., Tomita, N., Ohue, M. & Hayakawa, T. (1997). Microsatellite instability and mutated type II transforming growth factor-beta receptor gene in gliomas. *Cancer Lett*, *112*(2), 251–256.

Josefowicz, S. Z., Lu, L.-F., & Rudensky, A. Y. (2012). Regulatory T Cells: Mechanisms of Differentiation and Function. *Annu Rev Immunol*, *30*(1), 531–564.

Kalathil, S. G., Lugade, A. A., Miller, A., Iyer, R., and Thanavala, Y. (2013). Higher frequencies of GARP+CTLA4+Foxp3+ T regulatory cells and myeloid-derived suppressor cells in hepatocellular carcinoma patients are associated with impaired T cell functionality. *Cancer res*, *73*(8), 2435-2444.

Koebel, C. M., Vermi, W., Swann, J. B., Zerafa, N., Rodig, S. J., Old, L. J., Smyth, M. J., & Schreiber, R. D. (2007). Adaptive immunity maintains occult cancer in an equilibrium state. *Nature*, *450*(7171), 903–907.

Korah, J., Falah, N., Lacerte, A., & Lebrun, J. J. (2012). A transcriptionally active pRb-E2F1-P/CAF signaling pathway is central to TGFβ-mediated apoptosis. *Cell Death & Dis*, *3*(10), e407.

Kos, C. H. (2004). Cre/loxP system for generating tissue-specific knockout mouse models. *Nutr Rev*, *62*(6 Pt 1), 243–246.

Kubota, K., Kim, J. Y., Sawada, A., Tokimasa, S., Fujisaki, H., Matsuda-Hashii, Y., Ozono, K., & Hara, J. (2004). LRRC8 involved in B cell development belongs to a novel family of leucine-rich repeat proteins. *FEBS Lett*, *564*(1–2), 147–152.

Lacerte, A., Korah, J., Roy, M., Yang, X. J., Lemay, S., & Lebrun, J. J. (2008). Transforming growth factor-β inhibits telomerase through SMAD3 and E2F transcription factors. *Cell Signal*, *20*(1), 50–59.

Li, J. M., Nichols, M. A., Chandrasekharan, S., Xiong, Y., & Wang, X. F. (1995). Transforming growth factor beta activates the promoter of cyclin-dependent kinase inhibitor p15INK4B through an Sp1 consensus site. *J Biol Chem, 270*(45), 26750–26753.

Li, M. O., Wan, Y. Y., and Flavell, R. A. (2007). T cell-produced transforming growth factor-β controls T cell tolerance and regulates Th1- and Th17-cell differentiation. *Immunity*, *26*(5), 579-591.

Li, Y., Kim, B.-G., Qian, S., Letterio, J. J., Fung, J. J., Lu, L., & Lin, F. (2015). Hepatic Stellate Cells Inhibit T Cells through Active TGF-β1 from a Cell Surface-Bound Latent TGF-β1/GARP Complex. *J Immunol*, *195*(6), 2648–2656.

Liu, Y., Cox, S. R., Morita, T., & Kourembanas, S. (1995). Hypoxia regulates vascular endothelial growth factor gene expression in endothelial cells. Identification of a 5' enhancer. *Circ Res*, *77*(3), 638–643.

Loeb, K. R., & Loeb, L. A. (2000). Significance of multiple mutations in cancer. *Carcinogenesis*, *21*(3), 379–385.

Macaulay, I. C., Tijssen, M. R., Thijssen-Timmer, D. C., Gusnanto, A., Steward, M., Burns, P., Langford, C. F., Ellis, P. D., Dudbridge, F., Zwaginga, J. J., *et al*. (2007). Comparative gene expression profiling of in vitro differentiated megakaryocytes and erythroblasts identifies novel activatory and inhibitory platelet membrane proteins. *Blood*, *109*(8), 3260–3269.

Macey, M. G. (2007). Principles of flow cytometry. In: Macey, M. G. (Editor), *Flow Cytometry: Principles and Applications*, Humana Press Inc., 1–15.

Malinda, K. M. (2009). In vivo matrigel migration and angiogenesis assay. *Methods Mol Biol*, *467*, 287–294.

Massagué, J., Seoane, J., & Wotton, D. (2005). Smad transcription factors. *Gene Dev*, *19*(23), 2783-2810.

Medina-Echeverz, J., Fioravanti, J., Zabala, M., Ardaiz, N., Prieto, J., & Berraondo, P. (2011). Succesful colon cancer eradication after chemoimmunotherapy is associated with profound phenotypic change of intratumoral myeloid cells. *J Immunol*, *186*(2), 807-815.

Metelli, A., Wu, B. X., Fugle, C. W., Rachidi, S., Sun, S., Zhang, Y., Wu, J., Tomlinson, S., Howe, P. H., Yang, Y., *et al*. (2016). Surface expression of TGFβ docking receptor GARP promotes oncogenesis and immune tolerance in breast cancer. *Cancer res*, *76*(24): 7601-7617.

Moustakas, A., & Heldin, C.-H. (2005). Non-Smad TGF-beta signals. *J Cell Sci*, *118*(16), 3573-3784.

Nakamura, K., Kitani, A., Fuss, I., Pedersen, A., Harada, N., Nawata, H., & Strober, W. (2004). TGF-beta 1 plays an important role in the mechanism of CD4+CD25+ regulatory T cell activity in both humans and mice. *J Immunol*, *172*(2), 834–842.

Nishida, N., Yano, H., Nishida, T., Kamura, T., & Kojiro, M. (2006). Angiogenesis in cancer. *Vasc Health Risk Manag*, *2*(3), 213-219.

O'Connor, M. N., Salles, I. I., Cvejic, A., Watkins, N. A., Walker, A., Garner, S. F., Jones, C. I., Macaulay, I. C., Steward, M., Zwaginga, J. J., *et al*. (2009). Functional genomics in zebrafish permits rapid characterization of novel platelet membrane proteins. *Blood*, *113*(19), 4754–4762.

O'Kane, S., & Ferguson, M. W. J. (1997). Transforming growth factor βs and wound healing. *Int J Biochem Cell Biol*, *29*(1), 63–78.

Oleinika, K., Nibbs, R. J., Graham, G. J., & Fraser, A. R. (2013). Suppression, subversion and escape: The role of regulatory T cells in cancer progression. *Clin Exp Immunol*, *171*(1), 36–45.

Ollendorff, V., Szepetowski, P., Mattei, M.-G., Gaudray, P., & Birnbaum, D. (1992). New gene in the homologous human 11q13-q14 and mouse 7F chromosomal regions. *Mamm Genome*, *2*(3), 195–200.

Ollendorff, V., Noguchi, T., & Birnbaum, D. (1994). The GARP gene encodes a new member of the family of leucine-rich repeat-containing proteins*. Cell Growth Differ, 5*(2), 213–219.

Pandiyan, P., Zheng, L., Ishihara, S., Reed, J., & Lenardo, M. J. M. J. (2007). CD4+ CD25+ Foxp3+ regulatory T cells induce cytokine deprivation–mediated apoptosis of effector CD4+ T cells. *Nat Immunol*, *8*(12), 1353–62.

Park, K., Kim, S. J., Bang, Y. J., Park, J. G., Kim, N. K., Roberts, A. B., & Sporn, M. B. (1994). Genetic changes in the transforming growth factor beta (TGF-beta) type II receptor gene in human gastric cancer cells: correlation with sensitivity to growth inhibition by TGF-beta*. PNAS, 91*(19), 8772–8776.

Pastille, E., Bardini, K., Fleissner, D., Adamczyk, A., Frede, A., Wadwa, M., Von Smolinski, D., Kasper, S., Sparwasser, T., Gruber, A. D., *et al.* (2014). Transient ablation of regulatory T cells improves antitumor immunity in colitis-associated colon cancer. *Cancer Res*, *74*(16), 4258-4269.

Piccirillo, C. A., Letterio, J. J., Thornton, A. M., McHugh, R. S., Mamura, M., Mizuhara, H., & Shevach, E. M. (2002). CD4+CD25+ regulatory T cells can mediate suppressor function in the absence of transforming growth factor β1 production and responsiveness. *J Exp Med*, *196*(2), 237–245.

Potente, M., Gerhardt, H., & Carmeliet, P. (2011). Basic and therapeutic aspects of angiogenesis. *Cell*, *146*(6), 873-887.

Probst-Kepper, M., Geffers, R., Kröger, A., Viegas, N., Erck, C., Hecht, H. J., Lünsdorf, H., Roubin, R., Moharregh-Khiabani, D., Wagner, K., *et al*. (2009). GARP: A key receptor controlling FOXP3 in human regulatory T cells. *J Cell Mol Med*, *13*(9B), 3343–3357.

Qin, Z., Kim, H.-J., Hemme, J., & Blankenstein, T. (2002). Inhibition of methylcholanthrene-induced carcinogenesis by an interferon γ receptor-dependent foreign body reaction. *J Exp Med*, *195*(11), 1479-1490.

Qureshi, O. S., Zheng, Y., Nakamura, K., Attridge, K., Manzotti, C., Schmidt, E. M., Baker, J., Jeffery, L. E., Kaur, S., Briggs, Z., *et al*. (2011). Trans-endocytosis of CD80 and CD86: a molecular basis for the cell-extrinsic function of CTLA-4. *Science*, *332*(6029), 600–603.

Rachidi, S., Metelli, A., Riesenberg, B., Wu, B. X., Nelson, M. H., Wallace, C., Paulos, C. M., Rubinstein, M. P., Garrett-Mayer, E., Hennig, M., *et al*. (2017). Platelets subvert T cell immunity against cancer via GARP-TGFβ axis. *Sci Immunol*, *2*(11), eaai7911.

Randi, A. M., Laffan, M. A., & Starke, R. D. (2013). Von willebrand factor, angiodysplasia and angiogenesis. *Mediterr J Hematol Infect Dis, 5*(1), e2013060.

Ren, X., Ye, F., Jiang, Z., Chu, Y., Xiong, S., & Wang, Y. (2007). Involvement of cellular death in TRAIL/DR5-dependent suppression induced by CD4(+)CD25(+) regulatory T cells. *Cell Death Differ, 14*(12), 2076–2084.

Robertson, I. B., & Rifkin, D. B. (2013). Unchaining the beast; insights from structural and evolutionary studies on TGFβ secretion, sequestration, and activation. *Cytokine Growth Factor Rev*, *24*(4), 355-372.

Rolls, A., Shechter, R., London, A., Ziv, Y., Ronen, A., Levy, R., & Schwartz, M. (2007). Toll-like receptors modulate adult hippocampal neurogenesis. *Nat Cell Biol*, *9*(9), 1081–1088.

Roubin, R., Pizette, S., Ollendorff, V., Planche, J., Birnbaum, D., & Delapeyriere, O. (1996). Structure and developmental expression of mouse Garp, a gene encoding a new leucine-rich repeat-containing protein. *Int J Dev Biol*, *40*(3), 545–555.

Rubtsov, Y. P., Rasmussen, J. P., Chi, E. Y., Fontenot, J., Castelli, L., Ye, X., Treuting, P., Siewe, L., Roers, A., Henderson, W. R., *et al.* (2008). Regulatory T cell-derived interleukin-10 limits inflammation at environmental interfaces. *Immunity*, *28*(4), 546-558.

Sakaguchi, S. (2005). Naturally arising Foxp3-expressing CD25+CD4+ regulatory T cells in immunological tolerance to self and non-self. *Nat Immunol*, *6*(4), 345–352.

Sato, E., Olson, S. H., Ahn, J., Bundy, B., Nishikawa, H., Qian, F., Jungbluth, A. A., Frosina, D., Gnjatic, S., Ambrosone, C., *et al*. (2005). Intraepithelial CD8+ tumor-infiltrating lymphocytes and a high CD8+/regulatory T cell ratio are associated with favorable prognosis in ovarian cancer. *PNAS, 102*(51), 18538–18543.

Shankaran, V., Ikeda, H., Bruce, A. T., White, J. M., Swanson, P. E., Old, L. J., & Schreiber, R. D. (2001). IFNγ and lymphocytes prevent primary tumor development and shape tumor immunogenicity. *Nature*, *410*(6832), 1107–1111.

Shi, M., Zhu, J., Wang, R., Chen, X., Mi, L., Walz, T., & Springer, T. A. (2011). Latent TGF-β structure and activation. *Nature*, *474*(7351), 343–349.

Smyth, M. J., Thia, K. Y., Street, S. E. A., Cretney, E., Trapani, J. A., Taniguchi, M., Kawano, T., Pelikan, S. B., Crowe, N. Y., & Godfrey, D. I. (2000a). Differential tumor surveillance by natural killer (NK) and NKT cells. *J Exp Med*, *191*(4), 661–668.

Smyth, M. J., Thia, K. Y., Street, S. E., MacGregor, D., Godfrey, D. I., & Trapani, J. A. (2000b). Perforin-mediated cytotoxicity is critical for surveillance of spontaneous lymphoma. *J Exp Med*, *192*(5), 755–760.

Stahl, A., Connor, K. M., Sapieha, P., Chen, J., Dennison, R. J., Krah, N. M., Seaward, M. R., Willett, K. L., Aderman, C. M., Guerin, K. I., *et al*. (2010). The mouse retina as an angiogenesis model. *Invest Opthalmol Vis Sci*, *51*(6), 2813-2826.

Stanic, B., Van De Veen, W., Wirz, O. F., Rückert, B., Morita, H., Söllner, S., Akdis, C. A., & Akdis, M. (2015). IL-10-overexpressing B cells regulate innate and adaptive immune responses. *J Allergy Clin Immunol*, *135*(3), 771–780.

Starke, R. D., Ferraro, F., Paschalaki, K. E., Dryden, N. H., McKinnon, T. A. J., Sutton, R. E., Payne, E. M., Haskard, D. O., Hughes, A. D., Cutler, D. F., *et al.* (2011). Endothelial von Willebrand factor regulates angiogenesis. *Blood*, *117*(3), 1071-1080.

Stockis, J., Colau, D., Coulie, P. G., & Lucas, S. (2009a). Membrane protein GARP is a receptor for latent TGF-β on the surface of activated human Treg. *Eur J Immunol, 39*(12), 3315–3322.

Stockis, J., Fink, W., Francois, V., Connerotte, T., de Smet, C., Knoops, L., van der Bruggen, P., Boon, T., Coulie, P. G., & Lucas, S. (2009b). Comparison of stable human Treg and Th clones by transcriptional profiling. *Eur J Immunol*, *39*(3), 869–882.

Sun, L., Wu, G., Willson, J. K., Zborowska, E., Yang, J., Rajkarunanayake, I., Wang, J., Gentry, L. E., Wang, X. F., & Brattain, M. G. (1994). Expression of transforming growth factor beta type II receptor leads to reduced malignancy in human breast cancer MCF-7 cells. *J Biol Chem*, *269*(42), 26449–26455.

Tai, X., Van Laethem, F., Pobezinsky, L., Guinter, T., Sharrow, S. O., Adams, A., Granger, L., Kruhlak, M., Lindsten, T., Thompson, C. B., *et al.* (2012). Basis of CTLA-4 function in regulatory and conventional CD4+ T cells. *Blood*, *119*(22), 5155–5163.

ten Dijke, P., & Arthur, H. M. (2007). Extracellular control of TGFβ signaling in vascular development and disease. *Nat Rev Mol Cell Biol*, *8*(11), 857–869.

Thomas, L.; Discussion of cellular and humoral aspects of the hypersensitivity states. (1959) In: Lawrence HS, ed. Cellular and Humoral Aspects of Hypersensitivity. New York: Hoeber-Harper, 529–532.

Tian, M., & Schiemann, W. P. (2009). The TGF-beta paradox in human cancer: an update. *Future Oncol*, *5*(2), 259–271.

Torre, L., Bray, F., Siegel, R. L., Ferlay, J., Lortet-Tieulent, J., & Jemal, A. (2015). Global cancer statistics 2012. *CA Cancer J Clin*, *65*(2), 87-108.

Tran, D. Q., Andersson, J., Wang, R., Ramsey, H., Unutmaz, D., & Shevach, E. M. (2009). GARP (LRRC32) is essential for the surface expression of latent TGF-beta on platelets and activated FOXP3+ regulatory T cells. *PNAS*, *106*(32), 13445–13450.

Tsukada, T., Eguchi, K., Migita, K., Kawabe, Y., Kawakami, A., Matsuoka, N., Takashima, H., Mizokami, A., & Nagataki, S. (1995). Transforming growth factor beta 1 induces apoptotic cell death in cultured human umbilical vein endothelial cells with down-regulated expression of bcl-2. *Biochem Bioph Res Co*, *210*(3), 1076–1082.

Vandenbriele, C., Kauskot, A., Vandersmissen, I., Criel, M., Geenens, R., Craps, S., Luttun, A., Jansens, S., Hoylaerts, M. F., & Verhamme, P. (2015). Platelet endothelial aggregation receptor-1: A novel modifier of neoangiogenesis. *Cardiovasc Res*, *108*(1), 124–138.

Vermeersch, E., Denorme, F., Maes, W., De Meyer, S. F., Vanhoorelbeke, K., Edwards, J., Shevach, E., Unutmaz, D., Fujii, H., Deckmyn, H., & Tersteeg, C. (2017) The role of platelet and endothelial GARP in thrombosis and hemostasis. *PLoS ONE*, *12*(3), e0173329.

Vesely, M. D., Kershaw, M. H., Schreiber, R. D., & Smyth, M. J. (2011). Natural innate and adaptive immunity to cancer. *Annu Rev Immunol*, *29*, 235–271.

Wang, R., Wan, Q., Kozhaya, L., Fujii, H., & Unutmaz, D. (2008). Identification of a regulatory T cell specific cell surface molecule that mediates suppressive signals and induces Foxp3 expression. *PLoS ONE*, *3*(7).

Wang, R., Zhu, J., Dong, X., Shi, M., Lu, C., & Springer, T. A. (2012). GARP regulates the bioavailability and activation of TGFβ. *Mol Biol Cell*, *23*(6), 1129–1139.

Watkins, N. A., Gusnanto, A., De Bono, B., De, S., Miranda-Saavedra, D., Hardie, D. L., Angenent, W. G. J., Attwood, A. P., Ellis, P. D., Erber, W., *et al*. (2009). A HaemAtlas: Characterizing gene expression in differentiated human blood cells. *Blood*, *113*(19), e1-e9.

Wing, K., Onishi, Y., Prieto-Martin, P., Yamaguchi, T., Miyara, M., Fehervari, Z., Nomura, T., & Sakaguchi, S. (2008). CTLA-4 control over Foxp3+ regulatory T cell function. *Science*, *322*(5899), 271–275.

Yuan, L., Chan, G. C., Beeler, D., Janes, L., Spokes, K. C., Dharaneeswaran, H., Mojiri, A., Adams, W. J., Sciuto, T., Garcia-Cardeña, G., *et al.* (2016). A role of stochastic phenotype switching in generating mosaic endothelial cell heterogeneity. *Nat Commun*, *7*, 10160.

Yu, P., & Fu, Y. (2006). Tumor-infiltrating T lymphocytes: friends or foes? *Lab invest*, *86*(3), 231-245.

Zhang, B., Halder, S. K., Kashikar, N. D., Cho, Y.-J., Datta, A., Gorden, D. L., & Datta, P. K. (2010). Anti-metastatic role of Smad4 signaling in colorectal cancer. *Gastroenterology*, *138*(3), 969-980.e3.

Zhang, L., Conejo-Garcia, J. R., Katsaros, D., Gimotty, P. A., Massobrio, M., Regnani, G., Makrigiannakis, A., Gray, H., Schlienger, K., Liebman, M. N., *et al*. (2003). Intratumoral T cells, recurrence, and survival in epithelial ovarian cancer. *NEJM*, *348*(3), 203–213.

Zhang, X., Reddy, J., Ochi, H., Frenkel, D., Kuchroo, V. K., Weiner, H. L. (2006). Recovery from experimental allergic encephalomyelitis is TGF-beta dependent and associated with increases in CD4+LAP+ and CD4+CD25+ T cells. *Int Immunol, 18*(4), 495-503.

Zitvogel, L., Pitt, J. M., Daillère, R., Smyth, M. J., & Kroemer, G. (2016). Mouse models in oncoimmunology. *Nat Rev Cancer*, *16*(12), 759-773.

Appendix A - Risk analysis

The Laboratory for Thrombosis Research (Latron) at KU Leuven Kulak has a containment level L1. During experiments, a lab coat was always worn and products were carefully handled to avoid spatters and aerosols.

Gloves were worn when irritating or potentially carcinogenic products were used, such as Gelgreen, methyl green, acetone (E3), sodium hydroxide (E3), boric acid (E3), TBE (E4) and hydrogen peroxide (E4). Hydrogen peroxide was collected in a hydrogen peroxide waste container, VIP and acetone in a special waste container (category 5), methyl green residues in a halogenated organic waste container (category 4) and TBE residues in a non-halogenated organic waste container (category 3).

Special precautions were taken when MCA (E4) was used, since it is a strong carcinogenic substance. A mask, disposable lab coat, double gloves (with the first pair secured with tape) were worn. The MCA suspension was prepared under a hood. The hood where the experiments were carried out was lined with tape and covered with towel. All waste, needles, excess MCA, pipettes, lab coats and gloves were collected in the appropriate waste container. The bin was closed off and stored after the experiment.

Eukaryotic cell lines were handled under a laminar flow. Gloves and lab coat were always worn and especially when working with tryptan blue, which is a carcinogen. Work surfaces were regularly disinfected with servanol.

Mice experiments were performed during this master's thesis. The mice are housed in an A1 animalium. When entering the animalium, a special lab coat and gloves were worn to avoid scratch and bite wounds. Injections were performed according to the correct protocols of the Institutional Animal Care and Use Committee of KU Leuven (Belgium). Needles were thrown away in the appropriate waste containers and recapping of needles was forbidden. Sacrificing of the animals was done by administering an overdose of 5% isoflurane (E3) in O_2. Mice were laid in an anesthetic box connected to a waste gas scavenging system in order to contain the isoflurane and avoid the presence of isoflurane in the surroundings. Mice were killed by cervical dislocation and mouse carcasses were stored in a freezer until the specialized company Rendac collected them.

Appendix B - Breeding scheme

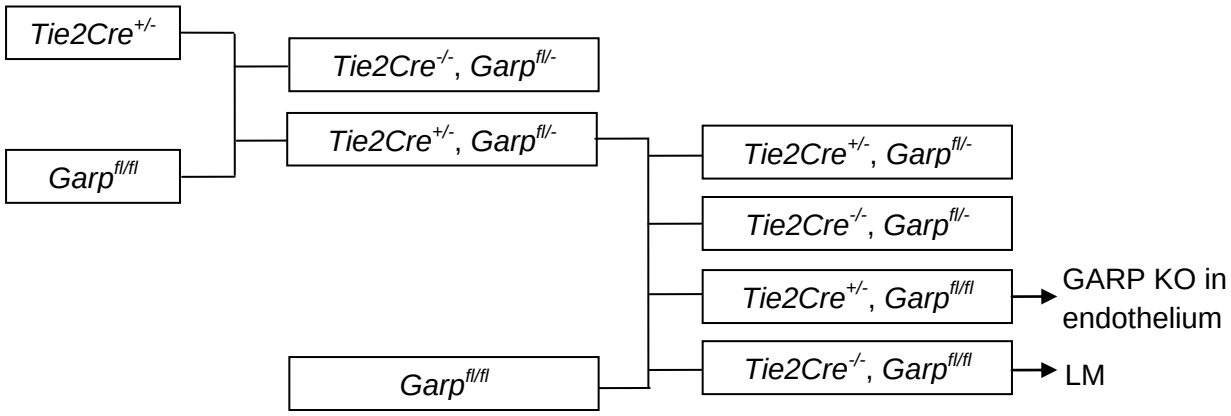

Figure 23: Schematic representation of the generation of *Tie2* specific GARP KO mice and controls. KO and LM mice were used in the experiments. Breeding scheme is identical for *Foxp3* mice.

AFDELING
Straat nr bus 0000
3000 LEUVEN, BELGIË
tel. + 32 16 00 00 00
fax + 32 16 00 00 00
www.kuleuven.be